Journal of Vibration Engineering & Technologies (2024) 12:5345–5368
https://doi.org/10.1007/s42417-023-00957-x

ORIGINAL PAPER

Three-Dimensional Thermal Vibration of CFFF Functionally Graded Carbon Nanotube-Reinforced Composite Plates

Bahar Uymaz[1] · **Gökay Uymaz**[2]

Received: 6 April 2022 / Revised: 10 August 2022 / Accepted: 24 March 2023 / Published online: 11 April 2023

Abstract

Purpose Three-dimensional thermal vibration analysis of functionally graded carbon nanotube (FG-CNT) reinforcement composite plates is performed for uniform, linear and sinusoidally temperature distribution.

Methods The reinforcement directions is considered through the thickness according to four reinforcement models as UD, FG-V, FG-O and FG-X are examined. As the components of the composite, the material properties of both the CNT forming the reinforcement phase and the polymer forming the matrix phase change depending on the temperature, and this is the focus of this study. The effective material properties of the FG-CNT reinforced composite are determined by the mixtures rule. The three displacements of the plates are expanded by a series of Chebyshev polynomials multiplied by appropriate functions to satisfy the essential boundary conditions. The natural frequencies are obtained by the Ritz method.

Results It is shown that the numerical results of the current approach are compared with the results of other researchers for validation, the results appear to be in good agreement. The effects of the thickness-to-length ratio and different volume fraction distributions for cantilever (CFFF) boundary conditions in considered thermal environments are investigated. The effect of different boundary conditions such as clamped (CCCC), simply supported (SSSS), simply supported through the x-axis and clamped through the y-axis (SCSC) and simply supported through the x-axis and free through the y-axis (SFSF) is also examined. It is shown that the increase in the amount of temperature and the type of temperature distribution are effective on the decrease of frequencies.

Keywords Thermal vibration · Thermal environment · Carbon nanotube-reinforced composite · Ritz method · Chebyshev polynomials

Introduction

Composites, which consist of two or more separate materials combined in a macroscopic structural unit, are made from various combinations of the other three materials. Composites are generally used because they have desirable properties which could not be achieved by either of the constituent materials acting alone. The most common example is the fibrous composite consisting of reinforcing fibers embedded in a binder, or matrix material. Particle or flake reinforcement is also used, but it is not so effective as fibers [1]. Advanced composites made from graphite, silicon carbide, aramid polymer, boron or other higher modulus fibers are used mainly in more exotic applications such as aerospace structures where their higher cost can be justified based on improved performance [1]. Graphite or carbon fibers are the most widely used advanced fibers, and graphite/epoxy or carbon/epoxy composites are now used routinely in aerospace structures. Although carbon fibers were once prohibitively expensive, the cost has dropped significantly as production capacity and demand has increased recent years. Polymers are unquestionably the most widely used matrix materials in modern composites. The application where the superior potential of high specific strength and high specific stiffness composites was first realized was in military aircraft, where performance and maneuverability are highly dependent on weight. However, composite structural elements are used in

✉ Bahar Uymaz
buymaz@nku.edu.tr

Gökay Uymaz
gokayuymaz@hattat.com.tr

[1] Engineering Faculty, Department of Mechanical Engineering, Tekirdağ Namık Kemal University, 59860 Çorlu, Tekirdağ, Turkey

[2] HEMA Endüstri A.Ş., Çerkezköy, Tekirdağ, Turkey

various components of automotive, aerospace, marine and architectural structures, as well as skis, golf clubs and it is also used in consumer products such as tennis rackets [1].

A new and rapidly developing field in nanomaterials science has started with the first time obtaining of the C_{60} molecule, which is formed by sixty carbon atoms taking the form of a soccer ball-shaped lattice structure, unlike crystal structures such as carbon, diamond and graphite [2]. Carbon nanotubes (CNTs) were first reported by Iijima [3], and it was demonstrated by Griebel and Hamaekers [4] that carbon can form a tube-shaped structure, with diameter ranges at nanoscale and lengths at micro scale.

Compared to carbon fiber-reinforced polymer composites, carbon nanotube-reinforced polymer composites have the potential to increase strength and stiffness and improve the structural, mechanical and electronic properties of the obtained composite due to CNTs low density and high aspect ratio [5–8]. Meguid and Sun [9] showed that the mechanical properties of the obtained composite would deteriorate if the CNT volume ratio exceeds a certain limit, and Han and Elliot [10] showed that the mechanical properties of the composite are also sensitive to the quantity and quality of the CNTs selected for the particular polymer. However, it was suggested to be used in the preferred direction in different gradients of CNT by Shen [11] to obtain nanocomposites desired performance. The fact that the mechanical properties of CNT and polymer change depending on temperature and that composite structures generally operate in high-temperature thermal environments have encouraged researchers to examine the behavior of CNT-reinforced polymer matrix composite structure components under mechanical and thermal loads for a high-quality design and production.

Three-dimensional thermoelastic analysis is researched by Alibeigloo and Liew [12] for FG-CNT/PmPV composite plates and by Alibeigloo [13] for FG-CNT/PmPV composite plates embedded in piezoelectric sensor and actuator layers. In both cases, the analyses are carried out using the Fourier series expansion and state-space method. Zhou and Song [14] studied three-dimensional nonlinear bending analysis of FG-CNT/PmPV composite plates using the element-free Galerkin method based on the S–R decomposition theorem. Zhu et al. [15] investigated bending and free vibration analyses of FG-CNT/PmPV composite plates by a finite element method based on the first-order shear deformation plate theory. For determination of the effective material properties of the considered plate, the rule of mixture is used. Static and free vibration analyses are carried out for FG-CNT/PmPV composite plates by Singh and Sahoo [16] using Navier's solution technique based on trigonometric shear deformation theory. Garcia-Macias et al. [17] investigated static and free vibration analyses of FG-CNT/PMMA composite skew plates using an efficient finite element formulation based on the Hu–Washizu principle. The used shell theory is formulated in oblique coordinates and includes the effects of transverse shear strains by first-order shear deformation plate theory. Wattanasakulpong and Chaikittiratana [18] presented an exact solution based on generalized shear deformation plat theory for static and dynamic analyses of FG-CNT/PmPV composite plates with Pasternak elastic foundation including shear layer and Winklersprings. Static response and free vibration of FG-CNT/PMMA composite plates resting on Winkler–Pasternak elastic foundations using Navier solution based on the first-order shear deformation plate theory is investigated by Duc et al. [19].

Lei et al. investigated free vibration [20] and buckling [21] of laminated FG-CNT/PmPV composite plates using kp-Ritz method based on first-order shear deformation theory. Malekzadeh and Zarei [22] investigated free vibration and Malekzadeh and Shojaee [23] investigated buckling behavior of quadrilateral laminated FG-CNT/PmPV composite plates by employing the differential quadrature method (DQM) based on the first-order shear deformation plate theory. Zhang et al. presented a free vibration analyses of FG-CNT/PmPV composite triangular plates [24] and buckling analysis of thick skew plates [25] using element-free IMSL-Ritz method based on the first-order shear deformation plate theory. For determination of the effective material properties of the considered plate, the rule of mixture is used. Zhang et al. [26] considered one more buckling analysis of FG-CNT/PmPV composite thick plates resting on Winkler foundations using element-free-based improved moving least squares-Ritz (IMLS-Ritz) method employed with first-order shear deformation theory. Farzam and Hassani [27] investigated thermal and mechanical buckling analysis of FG-CNT/PmPV composite plates using isogeometric analysis based on modified couple stress theory. Kiani [28] studied thermal shear buckling of FG-CNT/PMMA composite plates in uniform temperature distribution using the Ritz method with Chebyshev polynomials based on the first-order shear deformation theory. Kiani and Mirzaei [29] researched shear buckling of rectangular and skew FG-CNT/PMMA composite plates using the Ritz method whose shape functions are constructed according to the Gram–Schmidt process based on the first-order shear deformation theory. Mehrabadi et al. [30] investigated the mechanical buckling of a rectangular FG-CNT/PMMA composite plate reinforced by aligned and straight single-walled carbon nanotubes (SWCNTs) using the Mindlin plate theory considering the first-order shear deformation effect and variational approach. The material properties of SWCNT are determined according to molecular dynamics (MDs), and then the effective material properties at a point are estimated by either the Eshelby–Mori–Tanaka approach or the extended rule of mixture. Wu and Chang [31] considered a stability problem of FG-CNT/PmPV composite plates with surface-bonded piezoelectric actuator and sensor layers under bi-axial compression loads using a unified formulation of finite layer methods based on three-dimensional elasticity theory. Semi-analytical solutions to buckling and free vibration analysis of FG-CNT/PMMA composite thin plates applying the Galerkin technique with the classical plate theory presented by Wang et al. [32].

The free vibration analysis is considered for two directional FG-CNT/PmPV composite plates by Karamanlı and Aydoğdu [33] employing finite element method based on third-order shear deformation theory. A nonlinear vibration behaviors of FG-CNT/PMMA composite plates resting on an elastic foundation under uniform temperature distribution investigated by Wang and Shen [34] and the problem is solved by an improved perturbation technique based on a higher-order shear deformation plate theory. Guo and Zhang [35] studied the nonlinear oscillations and chaotic dynamics of a FG-CNT/PmPV composite plate subjected to the in-plane and the transverse excitations. The Galerkin method based on the Reddy's third-order shear deformation plate theory and the geometric nonlinearity of Von Karman. For determination of the effective material properties of the considered plate, Mori–Tanaka theory and the Eshelby's method are used. Quoc et al. [36] determined free vibration response of laminated piezoelectric FG-CNT/PMMA composite plates using the Navier technique based on a new four-variable refined plate theory. The free vibration of arbitrarily shaped FG-CNT/PMMA composite plates was considered by Fantuzzi et al. [37] by employing generalized Differential Quadrature Method based on the first-order shear deformation theory. The free vibration and bending analysis of graphene-reinforced composite circular and annular plates was considered by Bisheh et al. [38] by employing Differential Quadrature Method based on the three-dimensional elasticity theory. Shahrbabaki and Alibeigloo [39] applied the Ritz method to analyze free vibration based on three-dimensional elasticity theory. In this approach, orthogonal admissible functions were obtained from Jacobi polynomial. Effective material properties of the considered plate are estimated with the modified rule of mixture approach. Wang et al. [40] investigated free vibration and buckling behavior of FG-CNT-reinforced plates in the quadrilateral geometrical form by differential quadrature and finite element method based on the first-order shear deformation plate theory. Free vibration of regular and irregular plates with and without the temperature effect are considered for FG-CNT/PMMA composite plates and mechanical and thermal buckling considered for FG-CNT/PmPV composite plates under uniaxial and bi-axial in-plane load. Zhang et al. [41] considered free vibration of FG-CNT/PmPv composite plates subjected to in-plane loads using state-space Levy method based on Reddy's third-order shear deformation theory. Zhang and Selim [42] studied vibration analysis of FG-CNT/PmPV laminated thick composite plates employing element-free IMLS-Ritz method based on Reddy's higher-order shear deformation theory. The effective material properties of CNT-reinforced composite are estimated by a detailed and straightforward Mori–Tanaka approach.

Selim et al. [43] studied free vibration behavior of CNT-reinforced plates using element-free kp Ritz method based on Reddy's higher-order shear deformation theory. Parametric studies performed for FG-CNT/PmPV composite plates to reveal the effects of CNT distribution, boundary conditions, side to thickness ratio on natural frequencies and performed for FG-CNT/PMMA composite plates to reveal the effects of uniform temperature distribution on natural frequencies. The unified formulation of RMVT-based FPMs is extended to the free vibration analysis of FG-CNT-reinforced composite plates and laminated fiber-reinforced composite by Wu and Li [44]. Lei et al. [45] analyzed free vibration of FG-CNT-reinforced composite plates using element-free kp-Ritz method based on first-order shear deformation theory. In this study the effect of the uniform temperature distribution for $V_{CNT}^{*}=0.12$ volume fraction on UD and FG-V distributed composite on natural frequencies are obtained. Effective material properties of the considered plate are estimated with the Eshelby–Mori–Tanaka approach.

As mentioned in the literature, there are many studies on the bending, buckling and vibration behavior of CNT-reinforced plates. However, although the properties of both CNT and polymer materials that form the components of the CNT-reinforced composite, and thus the properties of the composite, vary depending on temperature, there are limited studies in which the effect of temperature is taken into account. This conclusion has been the inspiration for this study. In the present study, vibration analysis of FG-CNT/PmPV-reinforced composite plates in different thermal environments such as uniform, linear and sinusoidally temperature distribution are considered using Ritz method based on three-dimensional elasticity. The effective material properties of the considered plate are estimated by the rule of mixture. Chebyshev polynomials are assumed admissible functions in the Ritz method. However, scope of the study on cantilever (CFFF) boundary condition, different boundary conditions such as CCCC, SSSS, SCSC and SFSF are also examined. Parametric studies are performed for the thickness-to-length ratio, aspect ratio, uniform, linear and sinusoidally temperature fields and different volume fraction distributions.

Problem Formulation

Material properties of considered FG-CNT plate are assumed to be temperature dependent and reinforcement in thickness direction according to distribution as UD, FG-V,

Table 1 Temperature-dependent material properties of SWCNT at uniform temperature distribution in the thickness direction

T (K)	E_{11}^{CNT} (TPa)	E_{22}^{CNT} (TPa)	G_{12}^{CNT} (TPa)	α_{11}^{CNT} ($\times 10^{-6}$/K)	α_{22}^{CNT} ($\times 10^{-6}$/K)
300	5.6466	7.0800	1.9445	3.4584	5.1682
500	5.5308	6.9348	1.9643	4.5361	5.0189
700	5.4744	6.8641	1.9644	4.6677	4.8943
1000	5.2814	6.6220	1.9451	4.2800	4.7532

Table 2 Coefficients of the temperature-dependent material properties of SWCNT

Young modulus	P_0	P_1	P_2	P_3
E_{11}^{CNT} (TPa)	5.6466	-1.5849×10^{-4}	3.539×10^{-7}	-3.707×10^{-10}
E_{22}^{CNT} (TPa)	7.0800	-1.5852×10^{-4}	3.5408×10^{-7}	-3.709×10^{-10}
G_{12}^{CNT} (TPa)	1.9445	8.3093×10^{-5}	-1.7803×10^{-7}	8.5651×10^{-11}
α_{11}^{CNT} ($\times10^{-6}$ K)	3.4584	2.5039×10^{-3}	-5.3839×10^{-6}	3.2738×10^{-9}
α_{22}^{CNT} ($\times10^{-6}$ K)	5.1682	-1.5646×10^{-4}	6.0307×10^{-8}	-9.4442×10^{-13}
υ_{12}^{CNT}	0.175	0	0	0
ρ_{CNT} (kg/m^3)	1400	0	0	0

Table 3 Convergence and comparison of first six frequency parameters of SSSS square FG-CNT plates ($V_{CNT}{}^{*}=0.11$, UD, $\Delta T=0$)

$i\times j\times k$	Δ_1 (1,1)	Δ_2 (1,2)	Δ_3 (1,3)	Δ_4 (1,4)	Δ_5 (2,1)	Δ_6 (2,2)
$h/b=0.02$						
4×4×4	19.1592	25.0385	44.3595	85.0997	87.3396	95.9137
5×5×5	19.1592	23.2979	44.3245	70.2673	72.3720	83.0262
6×6×6	19.1540	23.2937	34.3767	70.2650	72.3698	77.9905
7×7×7	19.1540	23.2682	34.3764	53.6102	70.0169	72.1199
8×8×8	19.1540	23.2682	34.0363	53.6075	70.0169	72.1199
FSDT [15]	19.223	23.408	34.669	54.043	70.811	72.900
$h/b=0.1$						
4×4×4	13.5546	19.3452	19.4277	34.5079	34.6183	37.1525
5×5×5	13.5541	17.6866	19.4275	19.4275	32.9882	34.1846
6×6×6	13.5506	17.6838	19.4275	19.4275	27.4314	32.9215
7×7×7	13.5506	17.6582	19.4275	19.4275	27.4268	32.8920
8×8×8	13.5506	17.6582	19.4275	19.4275	27.1624	32.8916
FSDT [15]	13.532	17.700	19.449	19.449	27.569	32.563

FSDT first-order shear deformation theory

FG-O and FG-X models are examined. And also the reinforcement in thickness direction is examined of distribution as FG-V model in comparison study. In this study, thermal vibration in three different thermal environment with three-dimensional Ritz solution is performed.

Effective Material Properties of FG-CNT-Reinforced Composite Plates

The investigated FG-CNT reinforcement composite consists of CNT reinforcement phase that four type of distribution in the thickness direction and polymer matrix phase. The material properties both of two phases are assumed to be temperature dependent and reinforcement distribution models are assumed to be as uniform distribution (UD), V-type distribution (FG-V), O-type of distribution (FG-O) and X-type distribution (FG-X). The sum of volume fraction of reinforcement and matrix phases is

$$V_{CNT} + V_m = 1 \tag{1}$$

and the CNT volume fraction distributions in the thickness direction examined in the study are as follows.

Table 4 Comparison of natural frequency parameters of SSSS square FG-CNT/PMMA plates subjected to uniform temperature rise ($h/b = 0.1$, $V_{CNT}^* = 0.12$)

T^* (K)	Mode	UD			FG-V		
		Present	FSDT [45]	HSDT [34]	Present	FSDT [45]	HSDT [34]
300	Δ_1	12.2614	12.1261	12.2696	11.1577	11.3095	11.3074
	Δ_2	16.7718	16.5545	16.8071	16.1612	16.2611	16.1790
	Δ_3	17.0760	16.9835	–	17.1290	17.0406	–
	Δ_4	17.0760	26.0723	–	17.1290	25.9239	–
	Δ_5	26.6137	28.3715	29.4399	26.4141	27.8895	28.3821
	Δ_6	29.2190	30.6458	–	27.3959	29.9585	–
500	Δ_1	10.8741	10.9644	11.0402	9.9148	10.2442	10.2068
	Δ_2	14.4576	14.4941	14.7052	13.9884	14.2264	14.1873
	Δ_3	14.5431	14.5494	–	14.5032	14.5404	–
	Δ_4	14.5658	22.4220	–	14.6110	22.2866	–
	Δ_5	22.7962	25.0803	25.8619	22.5953	24.4494	25.1033
	Δ_6	25.2857	26.5461	–	23.7878	26.0737	–
700	Δ_1	8.9807	9.2518	9.3611	8.2287	8.7751	8.8190
	Δ_2	11.2497	11.5159	12.0533	11.2631	11.5436	11.6928
	Δ_3	11.5248	11.8279	–	11.2862	11.5514	–
	Δ_4	11.7202	17.9433	–	11.5605	17.8435	–
	Δ_5	18.1173	20.3060	21.3606	17.9344	19.9708	20.9137
	Δ_6	20.2049	21.3761	–	19.0960	21.1273	–

*T Top surface temperature of the plate, *HSDT* higher-order shear deformation theory

$$V_{\mathrm{CNT}}(z) = V_{\mathrm{CNT}}^{*} \quad (\mathrm{UD}) \tag{2}$$

$$V_{\mathrm{CNT}}(z) = V_{\mathrm{CNT}}^{*}\left(1 + 2\frac{z}{h}\right) \quad (\mathrm{FG\text{ - }V}) \tag{3}$$

$$V_{\mathrm{CNT}}(z) = 2V_{\mathrm{CNT}}^{*}\left(1 - 2\frac{z}{h}\right) \quad (\mathrm{FG\text{ - }O}) \tag{4}$$

$$V_{\mathrm{CNT}}(z) = 4V_{\mathrm{CNT}}^{*}\left(\frac{|z|}{h}\right) \quad (\mathrm{FG\text{ - }X}). \tag{5}$$

Here, the volume fraction of CNT (V_{CNT}^{*}) in the composite is defined as follows, based on the mass ratio of CNT.

$$V_{\mathrm{CNT}}^{*} = \frac{w_{\mathrm{CNT}}}{w_{\mathrm{CNT}} + \left(\frac{\rho^{\mathrm{CNT}}}{\rho^{\mathrm{m}}}\right) - \left(\frac{\rho^{\mathrm{CNT}}}{\rho^{\mathrm{m}}}\right) w_{\mathrm{CNT}}}, \tag{6}$$

where w_{CNT} is the mass fraction of the CNT in the FG-CNT composite. In the study, the mass fraction of CNT is the same in all reinforcement distribution models. The effective material properties such as Young modulus (E_{ii}), shear modulus (G_{ij}) and Poisson ratio (υ_{ij}) are defined according to the mixtures rule are given as follows.

$$E_{11}(z,\ T) = \eta_1 V_{\mathrm{CNT}}(z) E_{11}^{\mathrm{CNT}}(T) + V_{\mathrm{m}}(z)\, E^{\mathrm{m}}(T) \tag{7}$$

$$\frac{\eta_2}{E_{22}(z,\ T)} = \frac{V_{\mathrm{CNT}}(z)}{E_{22}^{\mathrm{CNT}}(T)} + \frac{V_{\mathrm{m}}(z)}{E^{\mathrm{m}}(T)} \tag{8}$$

$$\frac{\eta_3}{G_{12}(z,\ T)} = \frac{V_{\mathrm{CNT}}(z)}{G_{12}^{\mathrm{CNT}}(T)} + \frac{V_{\mathrm{m}}(z)}{G^{\mathrm{m}}(T)} \tag{9}$$

$$\nu_{12} = V_{\mathrm{CNT}}^{*}\, \nu_{12}^{\mathrm{CNT}} + V_{\mathrm{m}} \nu^{\mathrm{m}} \tag{10}$$

$$\nu_{21} = \nu_{12} \frac{E_{22}(z,\ T)}{E_{11}(z,\ T)} \tag{11}$$

$$\rho(z) = V_{\mathrm{CNT}}(z)\rho^{\mathrm{CNT}} + V_{\mathrm{m}}(z)\rho^{\mathrm{m}}, \tag{12}$$

where E_{ii}^{CNT} ($i, j = 1, 2, 3$) are the Young modulus, G_{ij}^{CNT} ($i, j = 1, 2, 3$) are the shear modulus, $\upsilon_{ij}^{\mathrm{CNT}}$ ($i, j = 1, 2, 3$) are the Poisson ratio of the CNTs in in-plane directions x and y and in thickness direction z, respectively. E^{m} is the Young modulus, G^{m} is the shear modulus, υ^{m} is the Poisson ratio of the isotropic matrix material. η_i ($i = 1, 2, 3$) are the size-dependent material properties. ρ^{CNT}, ρ^{m} and ρ are mass density per unit volume of CNT, matrix and FG-CNT composite, respectively. υ_{12} is considered as constant over the thickness of plate. The thermal coefficients (α_{ii}) ($i = 1, 2$) of the FG-CNT reinforcement composite are defined as,

$$\alpha_{11}(z,\ T) = V_{\mathrm{CNT}}(z)\alpha_{11}^{\mathrm{CNT}}(T) + V_{\mathrm{m}}(z)\alpha^{\mathrm{m}}(T) \tag{13}$$

Table 5 Natural frequency parameters of FG-CNT-reinforced plate with CFFF boundary condition ($a/b = 1$, $\Delta T = 0$)

Reinf. type	V_{CNT}^{*}	h/b	Δ_1	Δ_2	Δ_3	Δ_4	Δ_5	Δ_6
UD	0.11	0.05	6.3224	6.7283	10.1009	18.7523	19.7000	30.4975
		0.1	5.4306	5.7142	8.9462	9.3761	17.7965	20.2398
		0.2	3.7975	3.9396	4.6881	7.1248	12.0442	12.3033
	0.14	0.05	7.0237	7.3909	10.6271	19.1625	20.2171	32.7007
		0.1	5.8875	6.1337	9.2735	9.5812	18.1835	21.2420
		0.2	3.9851	4.1054	4.7906	7.2872	12.5068	12.7365
	0.17	0.05	7.7943	8.3121	12.5727	23.4463	24.6180	37.8128
		0.1	6.7205	7.0847	11.1607	11.7231	22.2541	25.1900
		0.2	4.7254	4.9087	5.8616	8.9076	15.0169	15.3487
FG-V	0.11	0.05	5.3022	5.8030	9.5999	18.7696	19.5596	26.8520
		0.1	4.7023	5.0789	8.6683	9.3850	17.7281	18.5298
		0.2	3.4641	3.6776	4.6852	7.0612	11.2510	11.6271
	0.14	0.05	5.8976	6.3581	10.0398	19.2197	20.0472	28.9945
		0.1	5.1309	5.4669	8.9711	9.6078	18.1331	19.5537
		0.2	3.6665	3.8532	4.7965	7.2286	11.7469	12.0911
	0.17	0.05	6.5159	7.1617	11.9818	23.5821	24.5275	33.2806
		0.1	5.8097	6.2996	10.8496	11.7864	22.2512	23.1244
		0.2	4.3177	4.5969	5.8835	8.8608	14.0789	16.5640
FG-O	0.11	0.05	4.6395	5.1883	9.0409	18.7933	18.8490	24.3591
		0.1	4.2073	4.6387	8.2808	9.3920	17.1867	17.4031
		0.2	3.2272	3.4828	4.6914	6.8613	10.7663	11.1790
	0.14	0.05	5.1723	5.6711	9.3734	19.1476	19.2399	26.4916
		0.1	4.6192	5.0011	8.5165	9.6154	17.4799	18.4778
		0.2	3.4445	3.6633	4.8034	6.9864	11.2911	11.6578
	0.17	0.05	5.7029	6.3845	11.1465	23.2552	23.6012	30.2604
		0.1	5.2047	5.7452	10.2449	11.7957	21.2869	21.8289
		0.2	4.0376	4.3570	5.8928	8.5144	13.5426	14.0424
FG-X	0.11	0.05	7.5058	7.8455	10.9958	18.7932	20.5883	33.7296
		0.1	6.1335	6.3509	9.3920	9.4451	18.3750	21.4924
		0.2	4.0254	4.1306	4.6914	7.3347	12.5274	12.7416
	0.14	0.05	8.2941	8.6036	11.6669	19.2398	21.3512	35.8024
		0.1	6.5750	6.7650	9.6154	9.8350	18.9294	22.4335
		0.2	4.1842	4.2775	4.8035	7.5445	12.9450	13.1439
	0.17	0.05	9.2554	9.7081	13.8463	23.6012	26.2355	41.7020
		0.1	7.5781	7.8707	11.7956	11.9242	23.3894	26.6508
		0.2	4.9920	5.1389	5.8929	9.2994	15.5803	15.8800

$$\begin{aligned}\alpha_{22}(z, T) = {} & (1 + \nu_{12}^{CNT})\, V_{CNT}(z)\alpha_{22}^{CNT}(T) \\ & + (1 + \nu^{m})\, V_{m}(z)\alpha^{m}(T) \\ & - \nu_{12}\alpha_{11}(z, T)\end{aligned} \tag{14}$$

where α_{ii}^{CNT} ($i, j = 1, 2, 3$) and α^{m} are the thermal coefficient of the CNTs in x and y directions, and isotropic matrix material, respectively. And the other effective material properties are assumed as, [13].

$$E_{33}(z, T) = E_{22}(z, T) \tag{15}$$

$$G_{23}(z, T) = G_{31}(z, T) = G_{12}(z, T) \tag{16}$$

$$\nu_{13} = \nu_{12} \tag{17}$$

$$\nu_{31} = \nu_{21} \tag{18}$$

$$\nu_{32} = \nu_{23} = \nu_{21} \tag{19}$$

Stress–Strain Relations Based on Three-Dimensional Elasticity

The considered moderately thick FG-CNT reinforcement plate in this paper is in the form of rectangular with length a,

Table 6 Natural frequency parameters of FG-CNT-reinforced plate with CFFF boundary condition ($a/b = 1.5$, $\Delta T = 0$)

Reinf. type	V_{CNT}^*	h/b	Δ_1	Δ_2	Δ_3	Δ_4	Δ_5	Δ_6
UD	0.11	0.05	6.5401	7.4914	17.4560	27.5552	35.5036	36.4854
		0.1	6.0494	6.8125	13.7776	16.4523	26.2420	27.0721
		0.2	4.8146	5.2590	6.8888	14.2724	16.4679	17.1396
	0.14	0.05	7.3149	8.1934	18.0105	28.2206	38.7399	39.5882
		0.1	6.6673	7.3522	14.1103	16.8895	27.8279	28.5841
		0.2	5.1472	5.5292	7.0552	14.5670	17.2026	17.8111
	0.17	0.05	8.0546	9.2636	21.7955	34.4388	43.8927	45.1515
		0.1	7.4670	8.4412	17.2194	20.5579	32.5992	33.6576
		0.2	5.9721	6.5435	8.6097	17.8501	20.5122	21.3690
FG-V	0.11	0.05	5.4403	6.5711	17.1913	27.6062	30.4701	31.7287
		0.1	5.1234	6.0698	13.7939	16.2960	23.5418	24.6042
		0.2	4.2562	4.8633	6.8862	14.2406	15.2335	16.1201
	0.14	0.05	6.0811	7.1405	17.6913	28.3239	33.4161	34.5629
		0.1	5.6649	6.5340	14.1517	16.7134	25.1360	26.1147
		0.2	4.5875	5.1273	7.0640	14.5491	15.9848	16.8128
	0.17	0.05	6.6768	8.1269	21.5429	34.6515	37.5949	39.2226
		0.1	6.3067	7.5278	17.3136	20.4398	29.2760	30.6468
		0.2	5.2771	6.0689	8.6418	17.8765	19.0392	20.1802
FG-O	0.11	0.05	4.7349	5.9431	16.4815	27.1038	27.6154	28.5019
		0.1	4.5133	5.5539	13.8018	15.7149	21.6982	22.8783
		0.2	3.8676	4.5731	6.8941	13.8425	14.4585	15.4136
	0.14	0.05	5.2982	6.4180	16.7965	28.3337	29.8785	31.1347
		0.1	5.0087	5.9579	14.1610	15.9805	23.3387	24.4013
		0.2	4.2010	4.8230	7.0739	14.0549	15.2332	16.1138
	0.17	0.05	5.8113	7.3071	20.3134	33.4755	34.6623	35.2101
		0.1	5.5586	6.8556	17.3249	19.4022	27.0787	28.5380
		0.2	4.8056	5.6924	8.6551	17.1470	18.1551	19.3329
FG-X	0.11	0.05	7.8749	8.7038	18.4387	27.6154	40.6382	41.3597
		0.1	7.0645	7.6889	13.8017	17.1767	28.4159	29.1241
		0.2	5.2892	5.6230	6.8940	14.6983	17.3306	17.8978
	0.14	0.05	8.7867	9.5600	19.2490	28.3336	43.8610	43.9080
		0.1	7.7234	8.2848	14.1609	17.7974	29.8858	30.5500
		0.2	5.5885	5.8802	7.0739	15.1218	18.0175	18.5444
	0.17	0.05	9.7060	10.8057	23.4624	34.6622	50.1704	51.2348
		0.1	8.7163	9.5475	17.3248	21.8603	35.1708	36.1274
		0.2	6.5440	6.9962	8.6551	18.7091	21.5175	22.2916

width b and thickness h. The origin of the coordinate system (x, y, z) is placed at the geometric center of the plate and the axes are parallel to the edges of the plate and the corresponding displacement components u, v and w along the x, y and z directions, respectively. For free vibration problem based on three-dimensional elasticity theory the displacement field is as follows

$$u\ (x,\ y,\ z;\ t) = U\ (x,\ y,\ z)\ e^{i\omega t} \tag{20}$$

$$v\ (x,\ y,\ z;\ t) = V\ (x,\ y,\ z)\ e^{i\omega t} \tag{21}$$

$$w\ (x,\ y,\ z;\ t) = W\ (x,\ y,\ z)\ e^{i\omega t} \tag{22}$$

where ω corresponds the natural frequency of the plate and $i = \sqrt{-1}$. The strain components ε_{ij} $(i, j = x, y, z)$ for small deformations are given as

$$\varepsilon_x = u_{,x} \tag{23}$$

$$\varepsilon_y = v_{,y} \tag{24}$$

$$\varepsilon_z = w_{,z} \tag{25}$$

Table 7 Natural frequency parameters of FG-CNT-reinforced plate under different boundary conditions at room temperature ($\Delta T = 0$, $h/b = 0.05$, $a/b = 1$)

Reinf. type	V_{CNT}^*	CCCC			SSSS			SCSC			SFSF		
		0.11	0.14	0.17	0.11	0.14	0.17	0.11	0.14	0.17	0.11	0.14	0.17
UD	Δ_1	28,5348	30,1369	35,4668	17,3111	18,9049	21,3968	18,3084	19,8508	22,6589	16,6694	18,3194	20,5850
	Δ_2	33,1181	34,6098	41,2389	21,4050	22,7900	26,5677	25,2017	26,5022	31,3502	16,9983	18,6137	21,0049
	Δ_3	43,8700	45,2873	54,7449	31,8427	33,0406	39,6955	38,5646	39,5488	48,1310	19,2036	20,6660	23,7988
	Δ_4	59,6824	62,2830	74,3275	38,8551	39,5488	48,6151	38,8551	39,7696	48,6151	26,3784	27,6132	32,8402
	Δ_5	60,7829	62,3452	75,9499	38,8551	39,5488	48,6151	52,6038	55,9375	65,3056	37,7006	38,5044	47,1425
	Δ_6	62,3785	64,9618	77,7215	49,8514	51,0997	62,2785	55,8644	58,6574	69,4235	38,8551	39,5488	48,6151
FG-V	Δ_1	25,8500	27,4876	32,1687	14,9621	16,3592	18,4680	16,1364	17,4743	19,9655	14,1617	15,6223	17,4457
	Δ_2	31,0030	32,5016	38,7031	19,7123	20,8971	24,5086	23,8339	24,9533	29,7336	14,5798	16,0030	17,9860
	Δ_3	42,5219	43,9391	53,2514	30,9358	31,9961	38,6975	37,8925	38,9912	47,4723	17,2571	18,5151	21,3981
	Δ_4	55,0349	57,8721	68,7329	38,9546	39,7254	48,9617	38,9546	39,7254	48,9617	25,1964	26,2653	31,4617
	Δ_5	58,1666	60,8975	72,6970	38,9546	39,7254	48,9617	46,9520	50,2814	58,3228	37,7732	38,6471	47,4410
	Δ_6	60,0651	61,5868	75,3458	46,5097	49,8613	57,7644	50,8492	53,9772	63,2814	38,9546	39,7254	48,9617
FG-O	Δ_1	23,8983	25,5745	29,7829	13,3747	14,6404	16,4857	14,6005	15,7856	18,0001	12,5079	13,8562	15,4204
	Δ_2	29,1968	30,6241	36,2853	18,2989	19,2824	22,5572	22,4889	23,3657	27,7479	12,9753	14,2751	15,9991
	Δ_3	40,7934	41,9780	50,5822	29,5722	30,3270	36,4834	36,5194	37,2684	45,1185	15,7828	16,8749	19,4632
	Δ_4	51,7642	54,8211	64,9387	38,9547	39,7256	48,9621	38,9547	39,7256	48,9621	23,8555	24,6717	29,4265
	Δ_5	55,0119	57,8806	68,8969	38,9547	39,7256	48,9621	43,0123	46,3851	53,5459	37,7835	38,6603	47,4562
	Δ_6	58,2589	59,3814	72,2013	42,5648	45,9669	52,9969	47,1454	50,2237	58,6263	38,9547	39,7256	48,8165
FG-X	Δ_1	30,6923	32,1025	38,0581	19,9118	21,6014	24,6148	20,8316	22,4968	25,8313	19,3588	21,0861	23,8808
	Δ_2	35,1517	36,5832	43,9216	23,6836	25,2575	29,5878	27,3358	28,8850	34,3403	19,6290	21,3310	24,2430
	Δ_3	45,8301	47,4053	57,7800	33,8200	35,3562	42,7617	38,9547	39,7256	48,9621	21,5892	23,1934	26,8425
	Δ_4	62,7961	64,7082	77,8947	38,9547	39,7256	48,9621	40,4874	42,0895	51,3010	28,4087	29,9093	35,7674
	Δ_5	62,8198	65,1191	79,5835	38,9547	39,7256	48,9621	57,2872	60,2382	70,8660	37,7833	38,6601	47,4560
	Δ_6	65,4008	67,7275	81,3363	51,8363	53,6043	65,8947	59,3036	61,1900	74,8449	38,9547	39,7256	48,9621

$$\gamma_{yz} = v_{,z} + w_{,y} \tag{26}$$

$$\gamma_{xz} = u_{,z} + w_{,x} \tag{27}$$

$$\gamma_{xy} = u_{,y} + v_{,x} \tag{28}$$

where $_{,(x,y,z)} = \left(\frac{\partial}{\partial x}, \frac{\partial}{\partial y}, \frac{\partial}{\partial z}\right)$. The stress–strain relations for a linear elastic orthotropic material are given by the generalized Hooke's law as follows

$$\sigma_x = C_{11}\varepsilon_x + C_{12}\varepsilon_y + C_{13}\varepsilon_z \tag{29}$$

$$\sigma_y = C_{12}\varepsilon_x + C_{22}\varepsilon_y + C_{23}\varepsilon_z \tag{30}$$

$$\sigma_z = C_{13}\varepsilon_x + C_{23}\varepsilon_y + C_{33}\varepsilon_z \tag{31}$$

$$\tau_{yz} = C_{44}\gamma_{yz} \tag{32}$$

$$\tau_{xz} = C_{55}\gamma_{xz} \tag{33}$$

$$\tau_{xy} = C_{66}\gamma_{xy} \tag{34}$$

where $[C]$ is stiffness matrix and its components are defined as follows

$$C_{11} = \frac{1 - \nu_{23}\nu_{32}}{E_2 E_3 \Delta} \tag{35}$$

$$C_{12} = \frac{\nu_{21} + \nu_{23}\nu_{31}}{E_2 E_3 \Delta} \tag{36}$$

$$C_{13} = \frac{\nu_{31} + \nu_{21}\nu_{32}}{E_2 E_3 \Delta} \tag{37}$$

$$C_{22} = \frac{1 - \nu_{13}\nu_{31}}{E_1 E_3 \Delta} \tag{38}$$

$$C_{23} = \frac{\nu_{32} + \nu_{12}\nu_{31}}{E_1 E_3 \Delta} \tag{39}$$

Table 8 Natural frequency parameters of FG-CNT-reinforced plate with CFFF boundary condition subjected to uniform temperature rise with $T_0 = 300$ K, $T_t = 500$ K ($a/b = 1$, UD)

V_{CNT}^*	h/b	Temp. distr.	Δ_1	Δ_2	Δ_3	Δ_4	Δ_5	Δ_6
0.11	0.05	Uniform	5.4173	5.6292	7.8279	13.9407	14.7192	25.1983
		Linearly	5.5882	5.8889	8.7090	16.4522	17.0290	27.7249
		Sinusoidally	5.6288	5.9463	8.8699	17.0569	17.4397	28.4020
	0.1	Uniform	4.6290	4.7577	6.8916	6.9703	13.3002	16.0404
		Linearly	5.0001	5.1960	7.8640	8.2404	15.4813	18.1688
		Sinusoidally	5.0963	5.3073	8.0605	8.5509	15.8874	18.7718
	0.2	Uniform	3.0038	3.0641	3.4851	5.3328	9.3096	9.4396
		Linearly	3.4161	3.5015	4.1290	6.2072	10.7292	10.8841
		Sinusoidally	3.5307	3.6222	4.2840	6.3874	11.1221	11.2822
0.14	0.05	Uniform	5.9679	6.1557	8.2552	14.2007	15.1209	26.6458
		Linearly	6.1873	6.4569	9.1605	16.7829	17.4685	29.5103
		Sinusoidally	6.2403	6.5256	9.3297	17.4091	17.8844	30.3013
	0.1	Uniform	4.9427	5.0511	7.1003	7.1330	13.5863	16.7143
		Linearly	5.3851	5.5519	8.1469	8.4042	15.8153	18.9946
		Sinusoidally	5.5014	5.6815	8.3557	8.7231	16.2323	19.6392
	0.2	Uniform	3.1151	3.1657	3.5502	5.4458	9.5997	9.7137
		Linearly	3.5642	3.6331	4.2118	6.3437	11.1015	11.2302
		Sinusoidally	3.6897	3.7630	4.3709	6.5299	11.5163	11.6488
0.17	0.05	Uniform	6.6970	6.9679	9.7458	17.4395	18.3950	31.3394
		Linearly	6.8979	7.2820	10.8444	20.5764	21.2846	34.4162
		Sinusoidally	6.9460	7.3514	11.0446	21.3308	21.7989	35.2560
	0.1	Uniform	5.7482	5.9137	8.6017	8.7197	16.6334	19.9967
		Linearly	6.1975	6.4495	9.8129	10.3065	19.3605	22.6321
		Sinusoidally	6.3140	6.5854	10.0570	10.6943	19.8678	23.3796
	0.2	Uniform	3.7468	3.8246	4.3598	6.6692	11.6236	11.7900
		Linearly	4.2559	4.3667	5.1642	7.7616	13.3869	13.5866
		Sinusoidally	4.3974	4.5161	5.3577	7.9865	13.8752	14.0820

$$C_{33} = \frac{1 - \nu_{12}\nu_{21}}{E_1 E_2 \Delta} \tag{40}$$

$$C_{44} = G_{23} \tag{41}$$

$$C_{55} = G_{31} \tag{42}$$

$$C_{66} = G_{12} \tag{43}$$

where Δ is defined as

$$\Delta = \left(1 - \nu_{12}\nu_{21} - \nu_{23}\nu_{32} - \nu_{13}\nu_{31} - 2\nu_{21}\nu_{32}\nu_{13}\right) / \left(E_1 E_2 E_3\right) \tag{44}$$

Thermal Analysis

In this study, thermal analysis is performed for FG-CNT reinforcement composite plates under uniform, linear and sinusoidal temperature rise through the thickness direction.

Uniform Temperature Rise

The temperature field under uniform temperature rise through the thickness is given as

$$T = T_0 + \Delta T, \tag{45}$$

where T_0 is the temperature of free stress state that $T_0 = 300$ K and ΔT denotes the temperature change.

Linear Temperature Rise

The temperature field under linear temperature rise through the thickness is given as

$$T = T_b + \Delta T\left(\frac{z}{h} + \frac{1}{2}\right), \tag{46}$$

where $\Delta T = T_t - T_b$ is the temperature gradient, T_b and T_t at the bottom and top of the plate, T_b equals the initial temperature 300 K.

Table 9 Natural frequency parameters of FG-CNT-reinforced plate with CFFF boundary condition subjected to uniform temperature rise with $T_0 = 300$ K, $T_t = 500$ K ($a/b = 1$, FG-V)

V_{CNT}^*	h/b	Temp. distr.	Δ_1	Δ_2	Δ_3	Δ_4	Δ_5	Δ_6
0.11	0.05	Uniform	4.3303	4.6223	7.2294	13.9489	14.5084	22.3303
		Linearly	4.4520	4.8512	8.1668	16.3105	16.9458	24.0623
		Sinusoidally	4.4822	4.9012	8.3297	16.8778	17.3942	24.6052
	0.1	Uniform	4.0326	4.2198	6.6215	6.9764	13.2292	14.7527
		Linearly	4.2762	4.5454	7.5733	8.1971	15.4273	16.3661
		Sinusoidally	4.3484	4.6359	7.7608	8.5078	15.8295	16.8949
	0.2	Uniform	2.7782	2.8788	3.4834	5.2791	8.7538	8.9590
		Linearly	3.0790	3.2207	4.1021	6.1399	9.8733	10.1335
		Sinusoidally	3.1754	3.3258	4.2577	6.3143	10.2300	10.4975
0.14	0.05	Uniform	4.7871	5.0524	7.5706	14.2416	14.8716	23.7911
		Linearly	4.9306	5.2972	8.5204	16.6517	17.3427	25.7656
		Sinusoidally	4.9685	5.3538	8.6887	17.2459	17.7897	26.3971
	0.1	Uniform	4.3451	4.5084	6.8530	7.1204	13.5231	15.4545
		Linearly	4.6324	4.8702	7.8310	8.3589	15.7746	17.1838
		Sinusoidally	4.7197	4.9741	8.0275	8.6780	16.1858	17.7543
	0.2	Uniform	2.9055	2.9929	3.5556	5.3987	9.0817	9.2676
		Linearly	3.2354	3.3595	4.1816	6.2824	10.2635	10.5030
		Sinusoidally	3.3425	3.4735	4.3413	6.4621	10.6416	10.8868
0.17	0.05	Uniform	5.3436	5.7207	9.0288	17.5390	18.1957	27.8420
		Linearly	5.4734	5.9914	10.2033	20.4456	21.2439	29.8997
		Sinusoidally	5.5070	6.0506	10.4051	21.1712	21.7865	30.5515
	0.1	Uniform	5.0123	5.2562	8.2951	8.7676	16.6108	18.4760
		Linearly	5.2954	5.6483	9.4881	10.2577	19.3817	20.4411
		Sinusoidally	5.3804	5.7571	9.7203	10.6460	19.8837	21.0939
	0.2	Uniform	3.4802	3.6106	4.3777	6.6285	10.9846	11.2479
		Linearly	3.8442	4.0337	5.1291	7.7150	12.3517	12.7021
		Sinusoidally	3.9622	4.1632	5.3235	7.9324	12.7940	13.1541

Sinusoidally Temperature Rise

The temperature field under sinusoidally temperature rise through the thickness is given as

$$T = T_b + \Delta T\left(1 - \cos\left(\frac{\pi}{2}\left(\frac{z}{h} + \frac{1}{2}\right)\right)\right), \tag{47}$$

where $\Delta T = \mathrm{T_t} - \mathrm{T_b}$ is the temperature gradient, T_b and T_t at the bottom and top of the plate, T_b equals the initial temperature 300 K.

Thermal Stresses Based on Three-Dimensional Elasticity

The plate is initially stress free at temperature T_0 and thermal stresses occur in the plate with temperature change. The initial stresses due to a temperature change of $\Delta T(z)$ are defined for an orthotropic plate as:

$$\sigma_x^T = -\left(C_{11}\alpha_1(z,\ T) + C_{12}\alpha_2(z,\ T)\right)\Delta T\ (z) \tag{48}$$

$$\sigma_y^T = -\left(C_{12}\alpha_1(z,\ T) + C_{22}\alpha_2(z,\ T)\right)\Delta T\ (z). \tag{49}$$

Three-Dimensional Ritz Solution in Thermal Environment

The linear elastic strain potential energy U_s of the plate can be given as,

$$U_s = \frac{1}{2}\int_V \left[\sigma_x\varepsilon_x + \sigma_y\varepsilon_x + \sigma_z\varepsilon_x + \tau_{yz}\gamma_{yz} + \tau_{xz}\gamma_{xz} + \tau_{xy}\gamma_{xy}\right] \mathrm{d}V. \tag{50}$$

The strain energy U_T from the initial stresses due to temperature rise can be given as,

$$U_T = \frac{1}{2}\int_V \left[\sigma_x^T d_{xx} + 2\tau_{xy}^T d_{xy} + \sigma_y^T d_{yy}\right] \mathrm{d}V \tag{51}$$

Table 10 Natural frequency parameters of FG-CNT-reinforced plate with CFFF boundary condition subjected to uniform temperature rise with $T_0 = 300$ K, $T_t = 500$ K ($a/b = 1$, FG-O)

V_{CNT}^*	h/b	Temp. distr.	Δ_1	Δ_2	Δ_3	Δ_4	Δ_5	Δ_6
0.11	0.05	Uniform	3.5845	3.9354	6.6807	13.9184	13.9714	20.3874
		Linearly	3.6772	4.1538	7.5811	16.1468	16.5528	22.0662
		Sinusoidally	3.6980	4.1973	7.7388	16.5516	17.1803	22.5261
	0.1	Uniform	3.6214	3.8476	6.3051	6.9819	12.8418	13.9327
		Linearly	3.8394	4.1657	7.2277	8.2540	14.9671	15.6636
		Sinusoidally	3.8958	4.2436	7.4072	8.5754	15.3648	16.1779
	0.2	Uniform	2.6221	2.7449	3.4876	5.1324	8.4116	8.6413
		Linearly	2.9306	3.1083	4.1291	5.9767	9.6253	9.9213
		Sinusoidally	3.0189	3.2088	4.2899	6.1492	9.9839	10.2889
0.14	0.05	Uniform	3.9756	4.2918	6.9245	14.1340	14.2594	21.8864
		Linearly	4.0883	4.5215	7.8299	16.3951	16.9045	23.8463
		Sinusoidally	4.1146	4.5692	7.9915	16.8034	17.5611	24.3923
	0.1	Uniform	3.9332	4.1289	6.4936	7.1261	13.0336	14.6713
		Linearly	4.1962	4.4822	7.4358	8.4341	15.1984	16.5554
		Sinusoidally	4.2655	4.5712	7.6231	8.7678	15.6041	17.1185
	0.2	Uniform	2.7640	2.8675	3.5599	5.2232	8.7669	8.9679
		Linearly	3.1098	3.2593	4.2196	6.0853	10.0619	10.3198
		Sinusoidally	3.2099	3.3694	4.3865	6.2637	10.4449	10.7101
0.17	0.05	Uniform	4.4258	4.8591	8.2448	17.1763	17.5576	25.5253
		Linearly	4.5245	5.1144	9.3491	19.9502	20.7739	27.5124
		Sinusoidally	4.5472	5.1655	9.5438	20.4432	21.5876	28.0558
	0.1	Uniform	4.5125	4.7947	7.8185	8.7748	15.8978	17.5528
		Linearly	4.7640	5.1726	8.9525	10.3705	18.5353	19.6935
		Sinusoidally	4.8292	5.2651	9.1742	10.7814	19.0296	20.3307
	0.2	Uniform	3.3017	3.4519	4.3837	6.3769	10.6104	10.8840
		Linearly	3.6779	3.8989	5.1880	7.4242	12.1248	12.4819
		Sinusoidally	3.7854	4.0225	5.3936	7.6396	12.5756	12.9442

$$d_{ij} = u_{,i}u_{,j} + v_{,i}v_{,j} + w_{,i}w_{,j} \quad (i,\ j = x,\ y). \tag{52}$$

The kinetic energy T_p of the plate can be given as:

$$T_p = \frac{1}{2}\int_V \rho\,(z,\ T)\left[\left(\frac{\partial u}{\partial t}\right)^2 + \left(\frac{\partial v}{\partial t}\right)^2 + \left(\frac{\partial w}{\partial t}\right)^2\right] \mathrm{d}V. \tag{53}$$

According to thermal vibration problem the maximum energy functional Π of the elastic plate is defined as:

$$\Pi = \left(U_{\text{smax}} + U_{\text{Tmax}}\right) - T_{\max}, \tag{54}$$

where U_{smax} is the nondimensionalized maximum of linear elastic strain potential energy, U_{Tmax} is the nondimensionalized maximum of thermal strain potential energy and $T_{\max}$ is the nondimensionalized maximum of kinetic energy. The nondimensionalization process is performed using the following nondimensionalized parameters:

$$X = 2x/a \tag{55}$$

$$Y = 2y/b \tag{56}$$

$$Z = 2z/h \tag{57}$$

Thus, the nondimensionalized maximum values of the energy equations are written as follows.

$$\begin{aligned} U_{\text{smax}} = \frac{h}{4\lambda}\int_{-1}^{1}\int_{-1}^{1}\int_{-1}^{1} \Big[& C_{11}\bar{\varepsilon}_x^2 + C_{22}\bar{\varepsilon}_y^2 + C_{33}\bar{\varepsilon}_z^2 \\ & + 2\left(C_{12}\bar{\varepsilon}_x\bar{\varepsilon}_y + C_{13}\bar{\varepsilon}_x\bar{\varepsilon}_z + C_{23}\bar{\varepsilon}_y\bar{\varepsilon}_z\right) \\ & + C_{44}\bar{\gamma}_{yz}^2 + C_{55}\bar{\gamma}_{xz}^2 + C_{66}\bar{\gamma}_{xy}^2 \Big]\, \mathrm{d}Z\,\mathrm{d}Y\,\mathrm{d}X \end{aligned} \tag{58}$$

$$\begin{aligned} U_{\text{Tmax}} = \frac{h}{4\lambda}\int_{-1}^{1}\int_{-1}^{1}\int_{-1}^{1} -\Big[& \left(C_{11}\alpha_1 + C_{12}\alpha_2\right)\Delta T\left\{\left(\frac{\partial U}{\partial X}\right)^2 + \left(\frac{\partial V}{\partial X}\right)^2 + \left(\frac{\partial W}{\partial X}\right)^2\right\} \\ & + \left(C_{12}\alpha_1 + C_{22}\alpha_2\right)\lambda^2\Delta T\left\{\left(\frac{\partial U}{\partial X}\right)^2 + \left(\frac{\partial V}{\partial X}\right)^2 + \left(\frac{\partial W}{\partial X}\right)^2\right\}\Big]\, \mathrm{d}Z\,\mathrm{d}Y\,\mathrm{d}X \end{aligned} \tag{59}$$

$$T_{\max} = \frac{abh}{16}\rho\omega^2\int_{-1}^{1}\int_{-1}^{1}\int_{-1}^{1}\left[U^2 + V^2 + W^2\right]\mathrm{d}Z\,\mathrm{d}Y\,\mathrm{d}X \tag{60}$$

Table 11 Natural frequency parameters of FG-CNT-reinforced plate with CFFF boundary condition subjected to uniform temperature rise with $T_0 = 300$ K, $T_t = 500$ K ($a/b = 1$, FG-X)

V_{CNT}^*	h/b	Temp. distr.	Δ_1	Δ_2	Δ_3	Δ_4	Δ_5	Δ_6
0.11	0.05	Uniform	6.5457	6.7067	8.6918	13.9714	15.4815	27.4527
		Linearly	6.8143	7.0490	9.6129	16.5031	17.8339	30.5130
		Sinusoidally	6.8791	7.1282	9.7861	17.1034	18.2382	31.3558
	0.1	Uniform	5.1245	5.2158	6.9819	7.2694	13.7350	16.9167
		Linearly	5.6204	5.7623	8.2543	8.3081	15.9794	19.2388
		Sinusoidally	5.7508	5.9041	8.5220	8.5548	16.3955	19.8853
	0.2	Uniform	3.1308	3.1748	3.4877	5.4796	9.6027	9.7084
		Linearly	3.5939	3.6507	4.1338	6.3809	11.1183	11.2289
		Sinusoidally	3.7220	3.7819	4.2832	6.5656	11.5293	11.6427
0.14	0.05	Uniform	7.1497	7.2925	9.2211	14.2594	16.0661	28.7747
		Linearly	7.4945	7.7057	10.1969	16.8644	18.4901	32.1778
		Sinusoidally	7.5790	7.8037	10.3848	17.4760	18.9075	33.1212
	0.1	Uniform	5.4049	5.4830	7.1261	7.5407	14.1394	17.5418
		Linearly	5.9807	6.1019	8.4348	8.6360	16.4524	20.0116
		Sinusoidally	6.1341	6.2652	8.7406	8.8649	16.8815	20.6956
	0.2	Uniform	3.2228	3.2625	3.5601	5.6267	9.8582	9.9573
		Linearly	3.7172	3.7645	4.2257	6.5558	11.4492	11.5437
		Sinusoidally	3.8540	3.9033	4.3777	6.7460	11.8789	11.9746
0.17	0.05	Uniform	8.0836	8.3005	10.9190	17.5575	19.7096	34.0051
		Linearly	8.4094	8.7243	12.0966	20.7351	22.7137	37.7587
		Sinusoidally	8.4886	8.8224	12.3149	21.4720	23.2217	38.7980
	0.1	Uniform	6.3436	6.4685	8.7748	9.1653	17.4774	21.0130
		Linearly	6.9505	7.1427	10.3714	10.4792	20.3292	23.8746
		Sinusoidally	7.1107	7.3179	10.7399	10.7463	20.8525	24.6723
	0.2	Uniform	3.8909	3.9547	4.3839	6.9478	11.9619	12.1142
		Linearly	4.4613	4.5433	5.1950	8.0861	13.8375	14.0009
		Sinusoidally	4.6191	4.7054	5.3783	8.3167	14.3445	14.5117

The above parameters are defined as follows:

$$\overline{\varepsilon}_X = \frac{\partial U}{\partial X} \tag{61}$$

$$\overline{\varepsilon}_y = \lambda \frac{\partial V}{\partial Y} \tag{62}$$

$$\overline{\varepsilon}_z = \frac{\lambda}{\gamma} \frac{\partial W}{\partial Z} \tag{63}$$

$$\overline{\gamma}_{xy} = \lambda \frac{\partial U}{\partial Y} + \frac{\partial V}{\partial X} \tag{64}$$

$$\overline{\gamma}_{yz} = \frac{\lambda}{\gamma} \frac{\partial V}{\partial Z} + \lambda \frac{\partial W}{\partial Y} \tag{65}$$

$$\overline{\gamma}_{zx} = \frac{\lambda}{\gamma} \frac{\partial U}{\partial Z} + \frac{\partial W}{\partial X} \tag{66}$$

and in here:

$$\lambda = a/b \tag{67}$$

$$\gamma = h/b. \tag{68}$$

In this thermal vibration problem of FG-CNT reinforcement plates, the Chebyshev polynomials are preferred which are the orthogonal polynomials reduced the computational effort [46]. In accordance with the Ritz method, each of the displacement amplitude functions is written as a triple series of Chebyshev polynomials, the displacement component of which is multiplied by a boundary function that satisfies the geometric boundary conditions of the plate. The displacement components are written in terms of nondimensionalized coordinates

$$U(X, Y, Z) = F_u(X, Y) \sum_{i=1}^{\infty} \sum_{j=1}^{\infty} \sum_{k=1}^{\infty} A_{ijk} P_i(X) P_j(Y) P_k(Z) \tag{69}$$

$$V(X, Y, Z) = F_v(X, Y) \sum_{l=1}^{\infty} \sum_{m=1}^{\infty} \sum_{n=1}^{\infty} B_{lmn} P_l(X) P_m(Y) P_n(Z) \tag{70}$$

$$W(X, Y, Z) = F_w(X, Y) \sum_{p=1}^{\infty} \sum_{q=1}^{\infty} \sum_{r=1}^{\infty} C_{pqr} P_p(X) P_q(Y) P_r(Z) \tag{71}$$

Table 12 Natural frequency parameters of FG-CNT-reinforced plate with CFFF boundary condition subjected to uniform temperature rise with $T_0 = 300$ K, $T_t = 500$ K ($a/b = 1.5$, UD)

V_{CNT}^*	h/b	Temp. distr.	Δ_1	Δ_2	Δ_3	Δ_4	Δ_5	Δ_6
0.11	0.05	Uniform	4.9216	5.4635	12.7116	20.5929	30.1993	30.2005
		Linearly	5.0087	5.7417	14.6061	24.2652	32.2951	32.9926
		Sinusoidally	5.0277	5.7909	14.9182	25.1608	32.8367	33.5766
	0.1	Uniform	5.2731	5.6542	10.2965	12.3577	21.2200	21.6733
		Linearly	5.5261	6.0783	12.1365	14.2675	23.7066	24.3214
		Sinusoidally	5.5883	6.1759	12.5842	14.6091	24.4047	25.0475
	0.2	Uniform	3.9786	4.1734	5.1482	10.6412	12.9210	13.2768
		Linearly	4.3992	4.6931	6.0789	12.3969	14.7394	15.2023
		Sinusoidally	4.5122	4.8297	6.3023	12.7303	15.2496	15.7322
0.14	0.05	Uniform	5.4763	5.9715	13.1083	21.0097	30.9577	32.4587
		Linearly	5.5904	6.2662	15.0318	24.7945	34.9890	35.4492
		Sinusoidally	5.6163	6.3209	15.3508	25.7184	35.6530	36.1714
	0.1	Uniform	5.7438	6.0757	10.5048	12.6954	22.2630	22.6765
		Linearly	6.0613	6.5492	12.4013	14.6470	24.9967	25.5552
		Sinusoidally	6.1406	6.6619	12.8631	14.9995	25.7687	26.3515
	0.2	Uniform	4.1893	4.3526	5.2524	10.8556	13.4078	13.7247
		Linearly	4.6706	4.9166	6.2121	12.6495	15.3443	15.7527
		Sinusoidally	4.8013	5.0671	6.4425	12.9916	15.8855	16.3112
0.17	0.05	Uniform	6.0759	6.7662	15.8796	25.7549	37.4652	37.6814
		Linearly	6.1755	7.1088	18.2500	30.3394	39.9934	40.8958
		Sinusoidally	6.1979	7.1694	18.6403	31.4569	40.6469	41.6032
	0.1	Uniform	6.5292	7.0171	12.8774	15.4428	26.4250	27.0018
		Linearly	6.8306	7.5368	15.1746	17.8299	29.4869	30.2705
		Sinusoidally	6.9050	7.6563	15.7332	18.2564	30.3466	31.1663
	0.2	Uniform	4.9509	5.2019	6.4387	13.3103	16.1177	16.5717
		Linearly	5.4651	5.8440	7.6006	15.5056	18.3728	18.9648
		Sinusoidally	5.6031	6.0125	7.8794	15.9222	19.0064	19.6236

where $P_s(\zeta) = \cos[(s-1)\arccos(\zeta)]$ $(s = 1, 2, 3, \ldots;$ $\zeta = X, Y, Z)$ is the sth order one-dimensional Chebyshev polynomial and $F_\alpha(X, Y) = f_\alpha^1(X, Y) f_\alpha^2(X, Y)$ $(\alpha = U, V, W)$ is the boundary function satisfying the geometric boundary conditions, are as follows in terms of nondimensionalized coordinates and Chebyshev polynomials. The boundary functions used for boundary condition in this study that CC ($f_u^{\,1}(X) = 1 - X^2$, $f_v^{\,1}(X) = 1 - X^2$, $f_w^{\,1}(X) = 1 - X^2$, $f_u^{\,2}(Y) = 1 - Y^2$, $f_v^{\,2}(Y) = 1 - Y^2$, $f_w^{\,2}(Y) = 1 - Y^2$); SS($f_u^{\,1}(X) = 1$, $f_v^{\,1}(X) = 1 - X^2$, $f_w^{\,1}(X) = 1 - X^2$; $f_u^{\,2}(Y) = 1 - Y^2$, $f_v^{\,2}(Y) = 1$, $f_w^{\,2}(Y) = 1 - Y^2$); CF ($f_u^{\,1}(X) = 1 + X$, $f_v^{\,1}(X) = 1 + X$, $f_w^{\,1}(X) = 1 + X$; $f_u^{\,2}(Y) = 1 + Y$, $f_v^{\,2}(Y) = 1 + Y$, $f_w^{\,2}(Y) = 1 + Y$) and FF ($f_u^{\,1}(X) = 1$, $f_v^{\,1}(X) = 1$, $f_w^{\,1}(X) = 1$; $f_u^{\,2}(Y) = 1$, $f_v^{\,2}(\mathrm{Y}) = 1$, $f_w^{\,2}(\mathrm{Y}) = 1$).

In accordance with the Ritz method, by substituting the displacement components given by Eq. (72) at the maximum energy values given by Eq. (59) and substituting the maximum energy values in the maximum energy functional given by Eq. (55), the energy functional Π is obtained in terms of Chebyshev polynomials. Then the energy functional Π is minimized according to the unknown coefficients A_{ijk}, B_{lmn} and C_{pqr}.

$$\frac{\partial \Pi}{\partial A_{ijk}} = 0 \tag{72}$$

$$\frac{\partial \Pi}{\partial B_{lmn}} = 0 \tag{73}$$

$$\frac{\partial \Pi}{\partial C_{pqr}} = 0 \tag{74}$$

As a result of the Ritz procedure, the eigenvalue problem given below is obtained, and the solution of the system of equations gives the natural frequencies of the free vibration problem occurring in the thermal environment under the influence of temperature.

Table 13 Natural frequency parameters of FG-CNT-reinforced plate with CFFF boundary condition subjected to uniform temperature rise with $T_0=300$ K, $T_t=500$ K ($a/b=1.5$, FG-V)

V_{CNT}^*	h/b	Temp. distr.	Δ_1	Δ_2	Δ_3	Δ_4	Δ_5	Δ_6
0.11	0.05	Uniform	3.3732	4.1849	12.3359	20.6300	25.7707	26.4552
		Linearly	3.4601	4.5135	14.3414	24.1645	27.1558	28.1128
		Sinusoidally	3.4768	4.5665	14.6582	25.0606	27.5616	28.5676
	0.1	Uniform	4.3942	4.9139	10.3073	12.1585	19.1717	19.7687
		Linearly	4.5607	5.2769	12.0804	14.1117	20.9619	21.7639
		Sinusoidally	4.6061	5.3625	12.5289	14.4504	21.5406	22.3780
	0.2	Uniform	3.5632	3.8576	5.1457	10.6060	11.9975	12.5027
		Linearly	3.8495	4.2676	6.0461	12.3775	13.4102	14.0582
		Sinusoidally	3.9380	4.3853	6.2708	12.7063	13.8675	14.5389
0.14	0.05	Uniform	3.7452	4.5088	12.6537	21.0873	27.8999	28.5052
		Linearly	3.8425	4.8437	14.7023	24.6890	29.5426	30.4123
		Sinusoidally	3.8635	4.9002	15.0264	25.6135	30.0387	30.9530
	0.1	Uniform	4.8166	5.2837	10.5355	12.4766	20.2426	20.7940
		Linearly	5.0163	5.6689	12.3411	14.4702	22.2201	22.9620
		Sinusoidally	5.0729	5.7639	12.8038	14.8177	22.8685	23.6416
	0.2	Uniform	3.7880	4.0444	5.2594	10.8298	12.5178	12.9818
		Linearly	4.1162	4.4847	6.1738	12.6456	14.0151	14.6189
		Sinusoidally	4.2196	4.6137	6.4055	12.9819	14.5026	15.1272
0.17	0.05	Uniform	4.1455	5.1886	15.4721	25.9179	31.9896	32.8761
		Linearly	4.2298	5.5920	18.0013	30.2313	33.5851	34.8284
		Sinusoidally	4.2474	5.6563	18.3963	31.3499	34.0603	35.3670
	0.1	Uniform	5.4366	6.1093	12.9489	15.2539	23.9625	24.7291
		Linearly	5.6222	6.5525	15.1107	17.7173	26.1208	27.1611
		Sinusoidally	5.6741	6.6561	15.6706	18.1392	26.8260	27.9125
	0.2	Uniform	4.4447	4.8286	6.4636	13.3181	15.0378	15.6873
		Linearly	4.7844	5.3365	7.5565	15.5599	16.7627	17.6166
		Sinusoidally	4.8905	5.4808	7.8370	15.9703	17.3292	18.2134

$$\left(\begin{bmatrix} [K_{uu}] & [K_{uv}] & [K_{uw}] \\ [K_{uv}]^T & [K_{vv}] & [K_{vw}] \\ [K_{uw}]^T & [K_{vw}]^T & [K_{ww}] \end{bmatrix} - \Omega^2 \begin{bmatrix} [M_{uu}] & 0 & 0 \\ 0 & [M_{vv}] & 0 \\ 0 & 0 & [M_{ww}] \end{bmatrix}\right) \begin{Bmatrix} \{A_{ijk}\} \\ \{B_{lmn}\} \\ \{C_{pqr}\} \end{Bmatrix} = \begin{Bmatrix} \{0\} \\ \{0\} \\ \{0\} \end{Bmatrix} \tag{75}$$

where $[K_{ij}]$ and $[M_{ij}]$ ($i, j=u, v, w$) are the stiffness matrix and diagonal mass matrix, respectively. The dimensionless coefficients $\{A_{ijk}\}$, $\{B_{lmn}\}$ and $\{C_{pqr}\}$ corresponding to the eigenvectors in the eigenvalue problem, represent the amplitude. Also, Ω is the non-dimensional frequency parameter and obtained as:

$$\Omega = \omega\,(a^2/h)\sqrt{\rho^{m0}/E^{m0}} \tag{76}$$

Here ω is the natural frequency and ρ^{m0} and E^{m0} are mass density per unit volume and Young modulus of matrix material at room temperature ($T_0=300$ K).

Numerical Results

In this study, a polymer matrix composite as defined Poly-*co*-vinylene (PmPV) reinforced by CNT in the thickness direction in three type of different form that UD, FG-V, FG-O and FG-X are examined. The mechanical properties of the matrix material PmPV, some of which are temperature dependent, are as follows [27]:

$$E^{\mathrm{m}} = (3.51 - 0.0047\ T)\ \mathrm{GPa} \tag{77}$$

$$\upsilon^{\mathrm{m}} = 0.34 \tag{78}$$

$$\rho^{\mathrm{m}} = 1150\ \mathrm{kg/m^3} \tag{79}$$

$$\alpha^{\mathrm{m}} = 45(1 + 0.0005\Delta T) \times 10^{-6}/\mathrm{K} \tag{80}$$

$$G^{\mathrm{m}} = \frac{E^{\mathrm{m}}}{2(1 + \nu^{\mathrm{m}})}\ \mathrm{GPa} \tag{81}$$

Table 14 Natural frequency parameters of FG-CNT-reinforced plate with CFFF boundary condition subjected to uniform temperature rise with $T_0 = 300$ K, $T_t = 500$ K ($a/b = 1.5$, FG-O)

V_{CNT}^*	h/b	Temp. distr.	Δ_1	Δ_2	Δ_3	Δ_4	Δ_5	Δ_6
0.11	0.05	Uniform	2.0788	3.2303	11.6907	20.6387	22.7610	23.5577
		Linearly	2.1471	3.5917	13.6098	23.9924	24.3182	25.0981
		Sinusoidally	2.1587	3.6461	13.9237	24.3072	25.2411	25.4724
	0.1	Uniform	3.7984	4.4089	10.3142	11.6872	17.8142	18.4828
		Linearly	3.9343	4.7718	12.1577	13.5679	19.6471	20.5526
		Sinusoidally	3.9672	4.8493	12.6210	13.9010	20.1716	21.1200
	0.2	Uniform	3.2738	3.6318	5.1518	10.3177	11.4198	11.9821
		Linearly	3.5464	4.0634	6.0810	12.0340	12.9526	13.6828
		Sinusoidally	3.6203	4.1736	6.3129	12.3603	13.4080	14.1654
0.14	0.05	Uniform	2.2922	3.3837	11.8394	21.0963	24.8090	25.5134
		Linearly	2.3752	3.7530	13.7852	24.8955	26.3031	27.2920
		Sinusoidally	2.3910	3.8105	14.1062	25.8607	26.6928	27.7339
	0.1	Uniform	4.1862	4.7327	10.5431	11.8910	18.9367	19.5389
		Linearly	4.3531	5.1126	12.4461	13.7941	21.0057	21.8204
		Sinusoidally	4.3944	5.1966	12.9293	14.1351	21.6056	22.4579
	0.2	Uniform	3.5107	3.8182	5.2665	10.4636	11.9693	12.4736
		Linearly	3.8307	4.2801	6.2256	12.2091	13.6114	14.2704
		Sinusoidally	3.9188	4.4008	6.4674	12.5427	14.1019	14.7847
0.17	0.05	Uniform	2.5466	3.9605	14.4005	25.9276	28.3232	29.3043
		Linearly	2.6131	4.3940	16.7686	29.7290	30.5382	31.0986
		Sinusoidally	2.6249	4.4593	17.1582	30.0894	31.5230	31.7282
	0.1	Uniform	4.7052	5.4637	12.9584	14.4385	22.3836	23.2003
		Linearly	4.8557	5.8980	15.2687	16.7609	24.6021	25.7177
		Sinusoidally	4.8925	5.9907	15.8600	17.1752	25.2357	26.4068
	0.2	Uniform	4.0987	4.5448	6.4735	12.7800	14.3941	15.0742
		Linearly	4.4214	5.0707	7.6374	14.9103	16.3005	17.1928
		Sinusoidally	4.5087	5.2047	7.9334	15.3168	16.8708	17.7976

The efficiency parameters of FG-CNT-reinforced composite are considered $\eta_1 = 0.149$ and $\eta_2 = \eta_3 = 0.934$ for VCNT* = 0.11; $\eta_1 = 0.150$ and $\eta_2 = \eta_3 = 0.941$ for VCNT* = 0.14; $\eta_1 = 0.149$ and $\eta_2 = \eta_3 = 1.381$ for VCNT* = 0.17. The temperature-dependent mechanical properties of the reinforcement material SWCNT which the type of armchair (10,10) are tabulated in Table 1 [27].

Using the data given in Table 1, the material properties of SWCNTs whose material properties depend on temperature were defined as a third-order polynomial as follows, thus provided the estimation of material properties at temperatures other than these:

$$P\ (T) = P_0\left(1 + P_1\Delta T + P_2\Delta T^2 + P_3\Delta T^3\right) \tag{82}$$

where P_0 is the material property of CNT at temperature T_0. P_0 and the coefficients of material properties depending on temperature, P_i ($i = 0$, 1, 2, 3) are given in Table 2 [27].

The material properties of the CNT reinforcement polymer matrix composite plate examined in the study are temperature dependent, and it has been reinforced in four different forms as UD, FG-V, FG-O and FG-X in the thickness direction. The investigated problem is the thermal vibration problem and three different thermal environments are taken into account.

Convergence and Accuracy Studies

In this study, the natural frequencies are obtained by Ritz method and the Chebyshev polynomials which defined between the interval [− 1, 1] and also by a set of separable orthogonal polynomial functions are used as admissible functions. This ensures more rapid convergence and better stability in the numerical computation can be accomplished compared with other polynomial series [46]. As it is known, the natural frequencies obtained by the Ritz method converge to the exact values from the upper bound and more accurate results can be obtained by increasing the number of terms of the admissible functions. In the current study, 3D solutions are obtained using Chebyshev polynomials with $8 \times 8 \times 8$ terms. The convergence study of SSSS square FG-CNT/PmPV composite with UD reinforcement in the stress-free temperature environment is performed for first six frequency parameters.

Table 15 Natural frequency parameters of FG-CNT-reinforced plate with CFFF boundary condition subjected to uniform temperature rise with $T_0 = 300$ K, $T_t = 500$ K ($a/b = 1.5$, FG-X)

V_{CNT}^*	h/b	Temp. distr.	Δ_1	Δ_2	Δ_3	Δ_4	Δ_5	Δ_6
0.11	0.05	Uniform	6.4790	6.8860	13.6653	20.6387	31.5482	34.1815
		Linearly	6.6203	7.1854	15.5781	24.3188	36.6014	37.0326
		Sinusoidally	6.6527	7.2435	15.8921	25.1873	37.4309	37.7816
	0.1	Uniform	6.1298	6.4138	10.3142	12.9500	22.7223	23.1051
		Linearly	6.5064	6.9316	12.1576	14.9224	25.5588	26.0752
		Sinusoidally	6.6005	7.0558	12.5910	15.2754	26.3540	26.8921
	0.2	Uniform	4.2755	4.4134	5.1519	10.9544	13.5028	13.7920
		Linearly	4.7938	5.0000	6.0849	12.7564	15.4680	15.8343
		Sinusoidally	4.9342	5.1566	6.3002	13.0965	16.0074	16.3894
0.14	0.05	Uniform	7.1787	7.5526	14.2823	21.0963	32.5591	36.3413
		Linearly	7.3670	7.8918	16.2505	24.8955	37.8256	39.6987
		Sinusoidally	7.4112	7.9610	16.5745	25.7835	38.6904	40.5959
	0.1	Uniform	6.6026	6.8497	10.5432	13.4142	23.6909	24.0496
		Linearly	7.0686	7.4436	12.4464	15.4559	26.7519	27.2335
		Sinusoidally	7.1869	7.5895	12.8895	15.8235	27.6119	28.1128
	0.2	Uniform	4.4535	4.5728	5.2667	11.2614	13.9432	14.2098
		Linearly	5.0306	5.2051	6.2310	13.1154	16.0257	16.3542
		Sinusoidally	5.1884	5.3759	6.4512	13.4649	16.5942	16.9359
0.17	0.05	Uniform	7.9974	8.5463	17.3852	25.9276	40.3344	42.2705
		Linearly	8.1672	8.9267	19.8380	30.5401	45.7595	46.2719
		Sinusoidally	8.2068	9.0005	20.2344	31.6039	46.6810	47.2479
	0.1	Uniform	7.5755	7.9582	12.9584	16.4633	28.1757	28.6947
		Linearly	8.0344	8.6038	15.2693	18.9780	31.6636	32.3606
		Sinusoidally	8.1497	8.7584	15.8002	19.4216	32.6447	33.3702
	0.2	Uniform	5.3009	5.4926	6.4736	13.9416	16.7927	17.1945
		Linearly	5.9368	6.2197	7.6442	16.2279	19.2188	19.7259
		Sinusoidally	6.1095	6.4137	7.9080	16.6548	19.8843	20.4117

Throughout the study, including the convergence and comparison studies, the non-dimensional frequency parameter Ω is taken as given in Eq. (26). As can be seen in Table 3, where the convergence rate of the first six frequency parameters is given, the convergence rate is good for each h/b ratio examined, and the variation of the frequency parameters decreases as the number of terms increases, and the frequency parameters approach a definite value.

The material examined in this study is FG-CNT/PmPV. However, FG-CNT/PMMA was taken into account in the comparison of the accuracy of the results obtained from the thermal vibration problem as it is available in the literature. The results given in Table 4 for SSSS square FG-CNT/PMMA composite are compared at uniform temperature rise. For this case, the assumed efficiency parameters dependent on SWCNT volume fraction for PMMA/CNT composite are taken from Wang and Shen [34] and, hence, for $V_{CNT}^* = 0.12$ are $\eta_1 = 0.137$, $\eta_2 = 1.022$ and $\eta_3 = 0.715$, $V_{CNT}^* = 0.17$ are $\eta_1 = 0.142$, $\eta_2 = 1.626$ and $\eta_3 = 1.138$ and $V_{CNT}^* = 0.28$ are $\eta_1 = 0.141$, $\eta_2 = 1.585$ and $\eta_3 = 1.109$. From the comparison results given in Tables 3 and 4, it is seen that the results obtained in this study are consistent and stable.

Parametric Studies

In the study is focused on to investigation effect of the temperature on frequency parameters in different thermal environment of Poly-*co*-vinylene (PmPV) matrix composite that reinforced by CNT in the thickness direction. The first six free vibration frequencies of the composite are obtained for the plate having CFFF, CCCC, SSSS, SCSC and SFSF boundary conditions at room temperature. The results are given in Tables 5, 6, 7. The first six free vibration frequencies of the composite are obtained for uniform temperature increase, linear temperature increase and sinusoidal temperature increase in the thickness direction when the lower surface of the plate at $T_b = T_0 = 300$ K and the upper surface of the plate at $T_t = 500$ K. The reinforcement modeling UD, FG-V, FG-O and FG-X of PmPV/FG-CNT plate at two side/side ratios 1 and 1.5, three different thickness/side ratios 0.05, 0.1 and 0.2 which corresponding, respectively, thin moderately thick and thick plates are considered for CFFF

Table 16 Natural frequency parameters of FG-CNT-reinforced plate under different boundary conditions with $T_0 = 300$ K, $T_t = 500$ K ($V_{CNT}^* = 0.11$, $h/b = 0.05$, $a/b = 1$)

		UD			FG-V			FG-O			FG-X		
		Uniform	Linear	Sinusoidal	Uniform	Linear	Sinusoidal	Uniform	Linear	Sinusoidal	Uniform	Linear	Sinusoidal
CCCC	Δ_1	22,9446	25,8019	26,5777	21,0110	23,1132	23,7513	19,6416	21,7502	22,3192	24,2294	27,5350	28,4400
	Δ_2	26,0246	29,5840	30,4509	24,4436	27,4300	28,1813	23,1405	26,1118	26,8062	27,2858	31,2394	32,2180
	Δ_3	33,5694	38,6731	39,7704	32,5037	37,2722	38,2860	31,2263	35,9221	36,8934	34,8618	40,2964	41,4801
	Δ_4	45,7720	53,1878	54,6862	43,4769	48,5128	50,1493	41,2830	46,6401	48,2076	47,1855	54,8964	56,4624
	Δ_5	46,7503	53,4060	55,2953	45,1566	51,1375	52,8362	43,3910	49,2825	50,9176	48,6438	55,8909	57,9310
	Δ_6	48,5376	55,6104	57,5471	45,5340	52,4210	53,8632	43,8076	50,9310	52,3394	50,4013	58,0342	60,1131
SSSS	Δ_1	15,0536	15,9920	16,2212	12,9233	13,6218	13,8030	11,4905	12,1298	12,2771	17,1322	18,3980	18,7165
	Δ_2	17,6044	19,2964	19,6492	15,9429	17,5523	17,8770	14,6606	16,2052	16,5046	19,4779	21,4214	21,8454
	Δ_3	24,7019	28,0595	28,6897	23,7027	27,1117	27,7289	22,5263	25,8202	26,4191	26,3367	29,8825	30,5616
	Δ_4	28,6118	34,0047	35,3356	28,6864	33,8870	35,2177	28,6865	34,0931	35,4681	28,6865	34,0927	35,3849
	Δ_5	28,8726	34,2242	35,5469	28,9465	34,1075	35,4298	28,9466	34,3121	35,6786	28,9466	34,3117	35,5960
	Δ_6	37,5994	43,5114	44,5980	37,1233	41,8895	42,9617	35,7039	39,0579	39,9924	39,1894	45,2882	46,4118
SCSC	Δ_1	15,6829	16,8051	17,0636	13,6704	14,6036	14,8210	12,2767	13,1500	13,3364	17,7171	19,1456	19,4883
	Δ_2	20,1739	22,4884	22,9469	18,7757	21,0655	21,5039	17,5664	19,7869	20,2050	21,9452	24,4771	24,9961
	Δ_3	28,8726	33,8453	34,6610	28,7240	33,1360	33,9427	27,5636	31,8461	32,6363	28,9466	34,3117	35,5960
	Δ_4	29,5099	34,2242	35,5469	28,9465	34,1075	35,4298	28,9466	34,3121	35,6786	31,0895	35,6031	36,4616
	Δ_5	43,0136	47,8951	49,2490	38,8349	42,2692	43,3537	35,9887	39,4243	40,3705	44,6559	51,7073	53,1290
	Δ_6	43,0784	50,0171	51,3271	41,2661	45,4560	46,6492	38,5499	42,7412	43,8088	45,8871	51,7822	53,3419
SFSF	Δ_1	14,6989	15,5042	15,7097	12,4666	12,9951	13,1477	10,9875	11,4465	11,5620	16,8306	17,9833	18,2822
	Δ_2	14,8599	15,7354	15,9545	12,6834	13,2959	13,4644	11,2382	11,7953	11,9290	16,9564	18,1667	18,4769
	Δ_3	16,1396	17,4499	17,7431	14,2845	15,4565	15,7152	12,9450	14,0529	14,2812	18,0832	19,6730	20,0453
	Δ_4	20,8346	23,3634	23,8565	19,5905	22,1234	22,5994	18,4051	20,8529	21,3070	22,5214	25,2511	25,8015
	Δ_5	27,9967	33,1154	34,3695	28,0464	32,9841	34,2395	28,0573	33,1876	34,4844	28,0571	33,1882	34,4043
	Δ_6	28,8726	34,2242	35,5469	28,9465	34,1075	35,4298	28,9466	34,3121	35,1944	28,9466	34,3117	35,5960

boundary condition and at side/side ratios 1, thickness/side ratios 0.05 are considered for CCC, SSSS, SCSC and SFSF boundary conditions. The results obtained for these conditions are given in Tables 8, 9, 10, 11, 12, 13, 14, 15, 16.

It is seen that the frequency values for the FG-X model are greater than the other models and the frequency values for the FG-O model are smaller than in all boundary conditions and the frequency values obtained at $a/b = 1.5$ ratio are greater than $a/b = 1$ ratio. However, the frequency values increase as the volume ratio increases and decrease as the thickness increases at the same volume ratio. At the same volume ratio and thickness values, with the increase of the a/b ratio, the amount of increase in the second and higher frequencies is greater than the amount of increase in the fundamental frequencies. For all reference parameters, the highest frequency values were obtained in the thermal environment where the temperature increased sinusoidally, and the lowest frequency values were obtained in the uniform temperature increase. The frequency values obtained in linear temperature variation were always obtained between the frequency values obtained from the uniform and sinusoidal temperature change.

When it is investigated according to boundary conditions, it is seen that the frequency values increase with increasing constraints on boundaries. And accordingly, the frequencies for each volume ratio are sorted from the highest to the lowest value according to boundary conditions CCCC, SCSC, SSSS, SFSF and CFFF, respectively.

The variation of the fundamental frequency parameters with temperature was investigated graphically for the 0.11, 0.14 and 0.17 values of the V_{CNT}^* while $h/b = 0.1$ and $a/b = 1$ in considered three thermal environments. Graphs are given in Fig. 1a–d for the reinforcement type that UD, FG-V, FG-O and FG-X, respectively. The curves show the effect of three different temperature distributions on the fundamental frequency parameters at each volume ratio. The fundamental frequency values for each volume ratio are higher for the reinforcement type that FG-X and the fundamental frequency values for each volume ratio are smaller for the reinforcement type that FG-O. The fundamental frequency values decrease as the temperature increases and show the greatest change in the uniform temperature distribution. In general, it is seen that the behavior of the material is more

Fig. 1 The fundamental frequency parameters of FG-CNT-reinforced plate with CFFF boundary condition ($h/b = 0.1$)

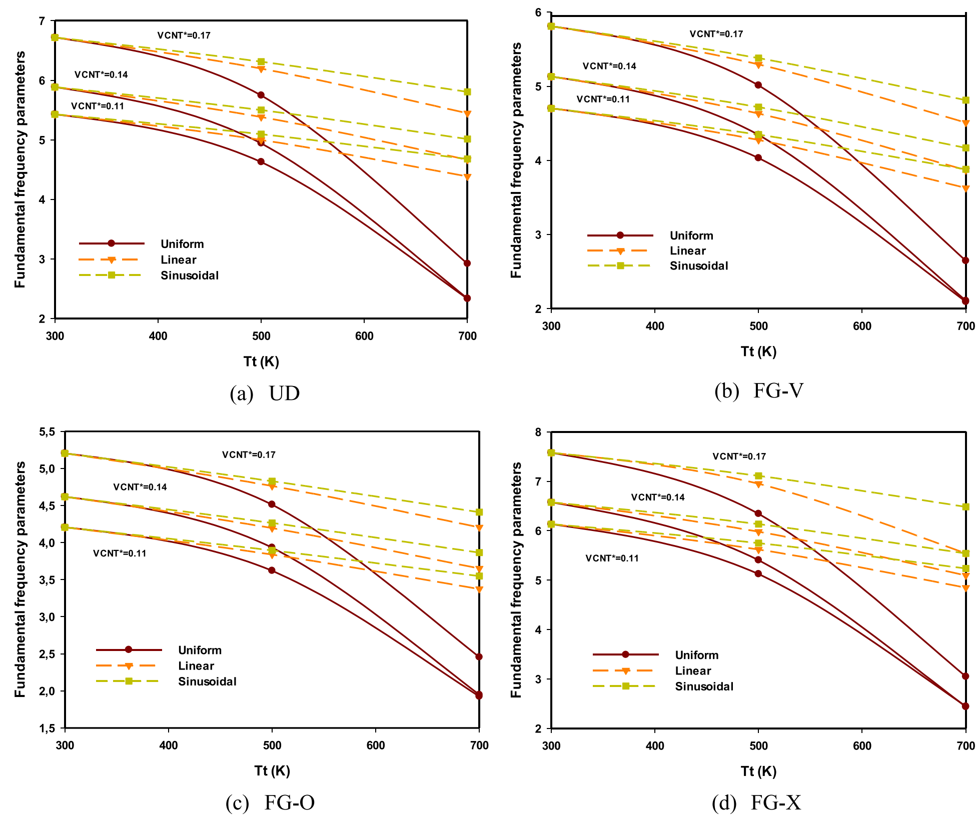

stable in the sinusoidal temperature distribution compared to other temperature distributions.

The greatest decrease in frequency values is observed in the uniform temperature distribution and the least decrease in the sinusoidal temperature distribution. When compared in terms of volume ratios, the rate of decrease in frequency value is higher at $V_{CNT}^{*} = 0.11$ for all boundary conditions. When compared in terms of fundamental frequency and high frequencies, the frequency that is least affected by temperature changes in all volume ratios is the fundamental frequency.

Figures 2, 3, 4, 5 show the mode shapes for the first 6 frequencies of the FG-CNT plate with CFFF boundary condition for all reinforcement models, at room temperature and uniform, linear and sinusoidal temperature increase. The mode shapes describe the deformation of the vertical component (W) of the FG-CNT composite plate when vibrating at natural frequency at room temperature and at different thermal environments. In the uniform temperature condition, fluctuations are observed in the nodal lines starting from the fourth frequency. In linear and sinusoidal temperature distribution, there is a tendency to increase in the number of waves starting from the fourth frequency.

Conclusions

The free vibration of FG-CNT/PmPV composite plate constructed by embedding a single wall carbon nanotube with chiral index (10,10) in different volume fractions into PmPV polymer matrices is investigated using Ritz method based on three-dimensional elasticity for three different thermal condition. Assumed thermal conditions are uniform, linear and sinusoidal temperature distribution in the study. The following conclusions can be carried out from the obtained results for the considered problem.

- The Chebyshev polynomials chosen as admissible functions in Ritz method provide high accuracy, consistent in the computation and rapid convergence.
- An increase in the volume ratio of CNT results in an increase in the natural frequency, and an increase in thickness at the same volume ratio results in a decrease in the natural frequency.
- The greatest and smallest frequency values for the reinforcement models were obtained for the FG-X model and for the FG-O model, respectively.
- The frequencies for each volume ratio are sorted from the highest to the lowest value according to boundary conditions CCCC, SCSC, SSSS, SFSF and CFFF, respectively.
- An increase in temperature causes the natural frequency to decrease.

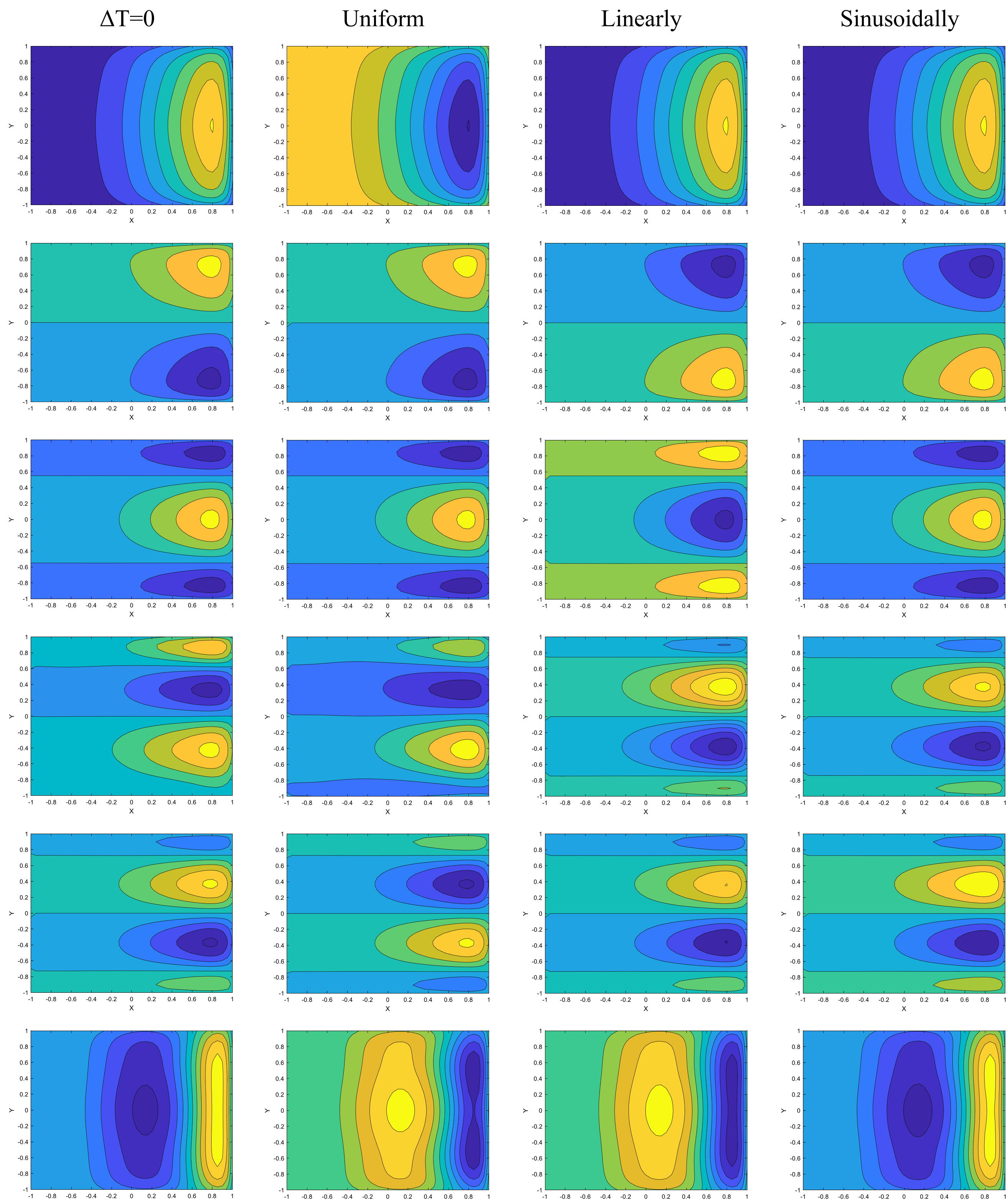

Fig. 2 First six mode shapes of square FG-CNT-reinforced plate with CFFF boundary condition (UD, $V_{\mathrm{CNT}}^{*}=0.14$, $h/b=0.05$, $T_{\mathrm{b}}=300$ K, $T_{\mathrm{t}}=500$ K)

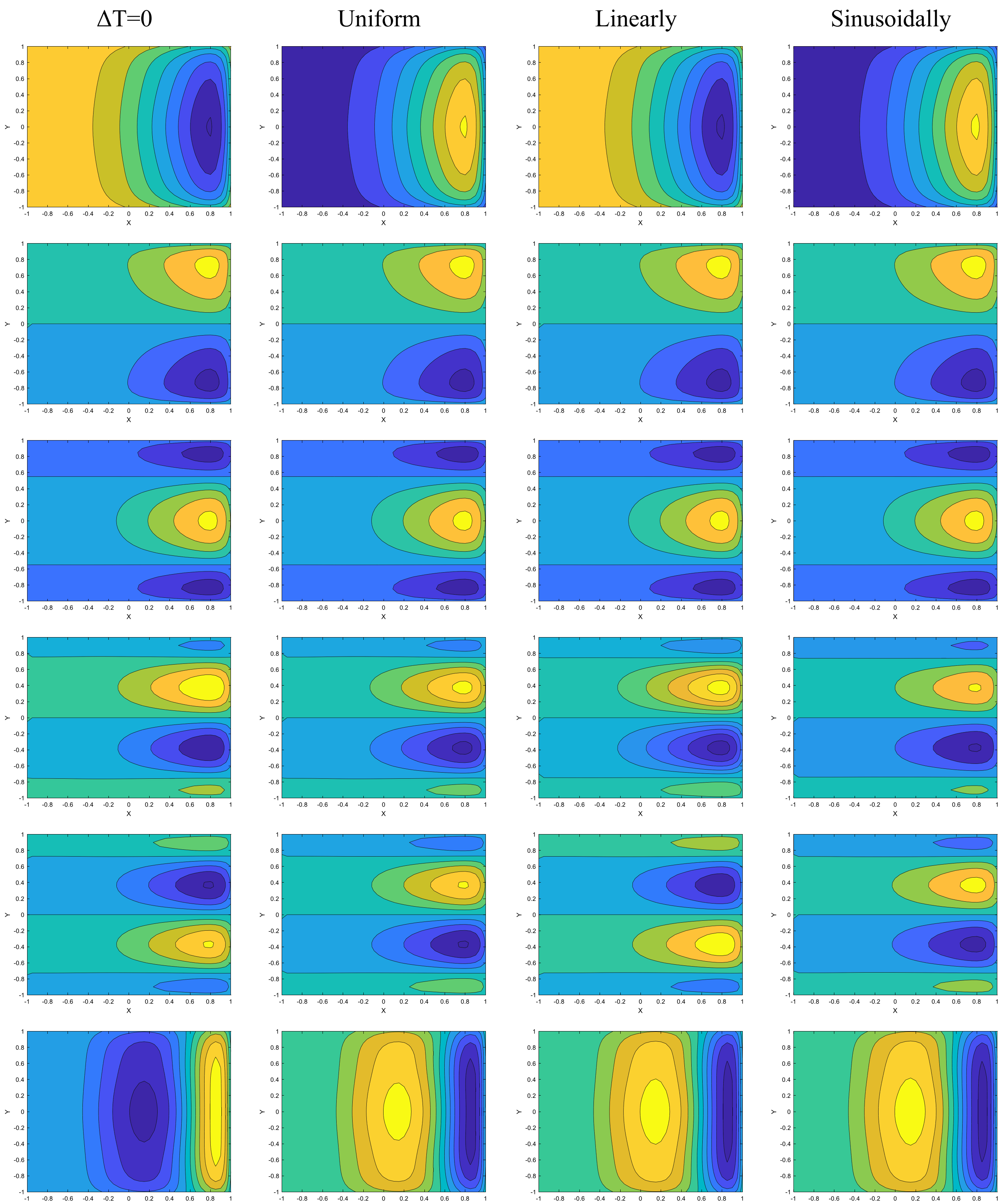

Fig. 3 First six mode shapes of square FG-CNT-reinforced plate with CFFF boundary condition (FG-V, $V_{CNT}^{*}=0.14$, $h/b=0.05$, $T_{b}=300$ K, $T_{t}=500$ K)

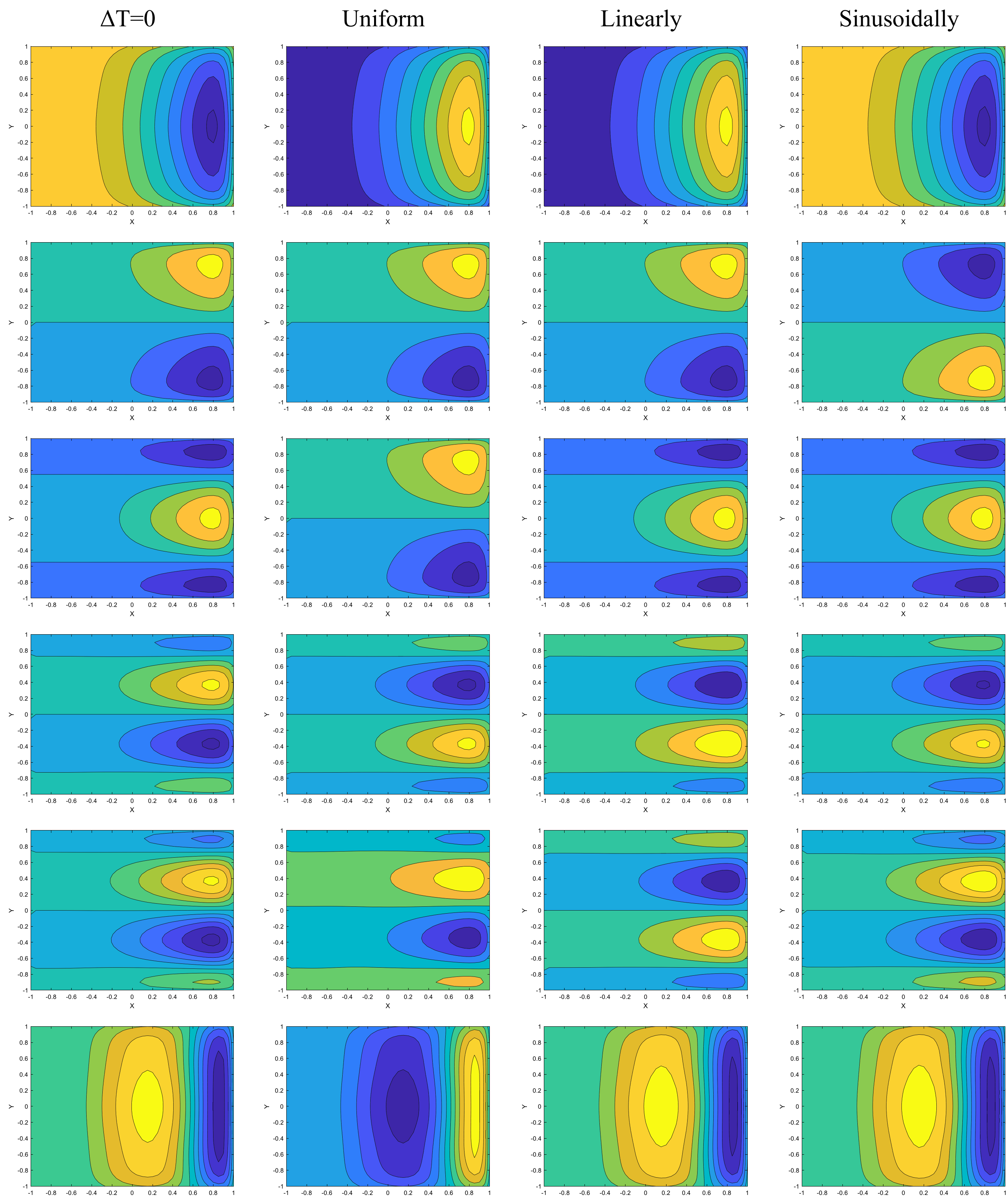

Fig. 4 First six mode shapes of square FG-CNT-reinforced plate with CFFF boundary condition (FG-O, $V_{CNT}^*=0.14$, $h/b=0.05$, $T_b=300$ K, $T_t=500$ K)

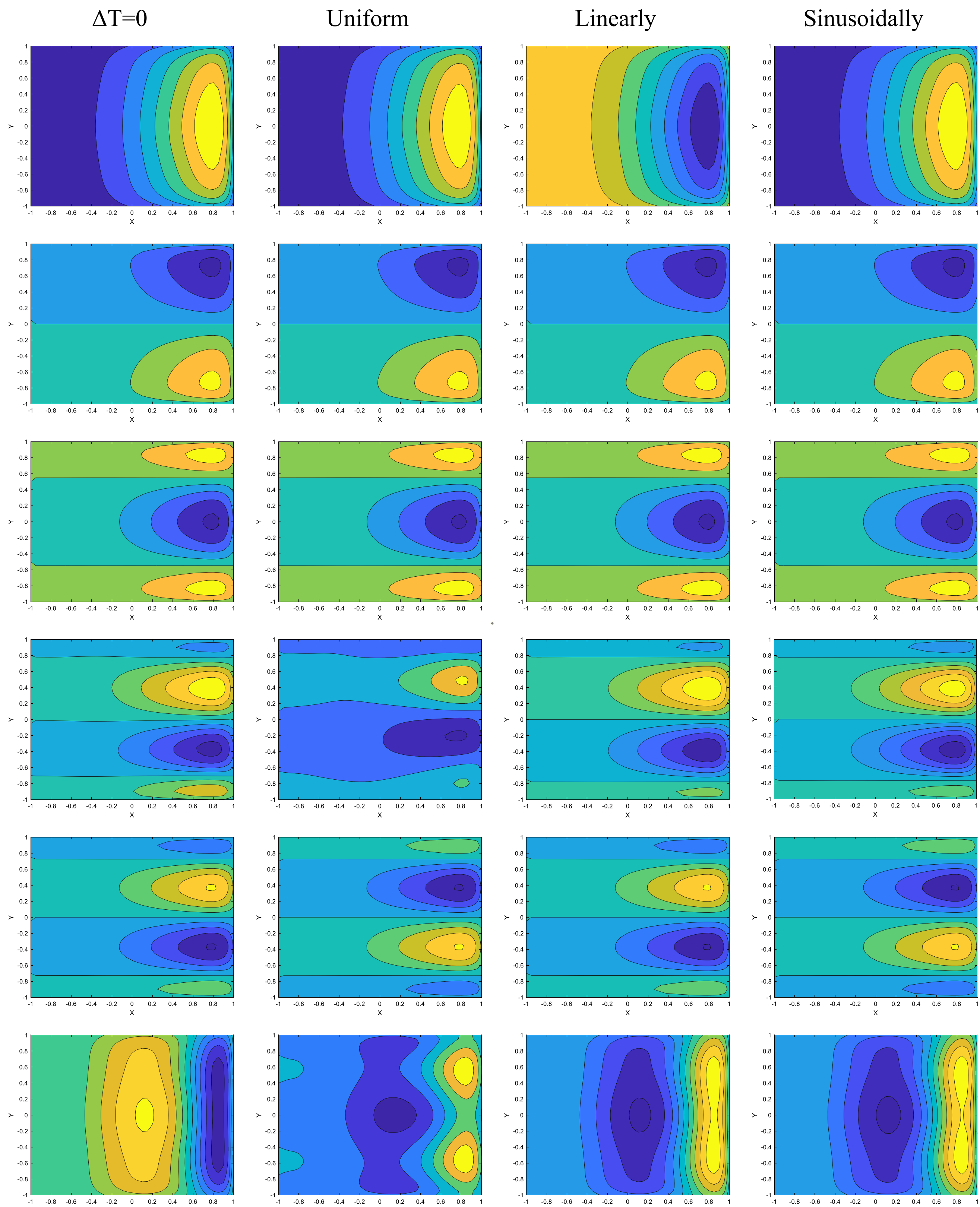

Fig. 5 First six mode shapes of square FG-CNT-reinforced plate with CFFF boundary condition (FG-X, $V_{CNT}^{*}=0.14$, $h/b=0.05$, $T_b=300$ K, $T_t=500$ K)

- The greatest and smallest frequency values for the three thermal conditions examined were obtained in sinusoidal and uniform temperature distribution, respectively.
- It is observed that in the uniform temperature distribution, frequencies sharply decrease and in the sinusoidal temperature distribution, frequencies monotonically decrease.
- The frequencies obtained in the linear temperature distribution were greater than the values obtained in the uniform temperature distribution and smaller than the values obtained in the sinusoidal temperature distribution for each condition. However, the variation of frequencies are more similar to the behavior in the sinusoidal temperature condition.
- As the temperature increases, the frequency decreases, and decrease ratio of frequency always higher at the lowest volume ratio of the CNT.
- For given boundary condition and at a certain temperature, in the change of temperature distributions, changes are also observed in the order of the mode shapes.
- Mode shapes are not greatly affected by the reinforcement model and temperature, but the greatest irregularity is seen in the FG-X model and uniform temperature distribution.

Funding The authors received no financial support for the research, authorship, and/or publication of this article.

Data availability The authors confirm that the data supporting the findings of this study are available within the article [and/or] its supplementary materials.

Declarations

Conflict of Interest The authors declare that no conflicts of interest exist with respect to the research, authorship, and/or publication of this article.

References

1. Gibson RF (2016) Principles of composite material mechanics. CRC Press, New York
2. Kroto HW, Heath JR, O'Brien SC, Curl RF, Smalley RE (1985) C60 buckminsterfullerene. Nature 318:162–163
3. Iijima S (1991) Helical microtubules of graphitic carbon. Nature 354:56–58
4. Griebel M, Hamaekers J (2004) Molecular dynamics simulations of the elastic moduli of polymer-carbon nanotube composites. Comput Methods Appl Mech Eng 193:1773–1778
5. Lau KT, Hui D (2002) The revolutionary creation of new advanced materials-carbonnanotube composites. Compos B Eng 33:263–277
6. Shirasu K, Nakamura A, Yamamoto G, Ogasawara Y, Shimamura Y, Inoue Y, Hashida T (2017) Potential use of CNTs for production of zero thermal expansion coefficient composite materials: An experimental evaluation of axial thermal expansion of CNTs using a combination of thermal expansion and uniaxial tensile tests. Compos A Appl Sci Manuf 95:152–160
7. Hassanzadeh-Aghdam MK, Mahmoodi MJ (2018) Micromechanical modelling of thermal conducting behavior of general carbon nanotube-polymer nanocomposites. Mater Sci Eng B 229:173–183
8. Sun CH, Li F, Cheng HM, Lu GQ (2005) Axial Young's modulus prediction of singlewalled carbon nanotubes arrays with diameters from nanometer to meterscales. Appl Phys Lett 87:193101–193104
9. Meguid SA, Sun Y (2004) On the tensile and shear strength of nano-reinforced composite interfaces. Mater Design 25:289–296
10. Han Y, Elliot J (2007) Molecular dynamics simulations of the elastic properties of polymer/carbon nanotube composites. Comput Mater Sci 39:315–323
11. Shen HS (2009) Nonlinear bending of functionally graded carbon nanotube-reinforced composite plates in thermal environments. Compos Struct 91:9–19
12. Alibeigloo A, Liew KM (2013) Thermoelastic analysis of functionally graded carbon nanotube-reinforced composite plate using theory of elasticity. Compos Struct 106:873–881
13. Alibeigloo A (2014) Three-dimensional thermoelasticity solution of functionally graded carbon nanotube reinforced composite plate embedded in piezoelectric sensor and actuator layers. Compos Struct 118:482–495
14. Zhou T, Song Y (2019) Three-dimensional nonlinear bending analysis of FG-CNTs reinforced composite plates using the element-free Galerkin method based on the S-R decomposition theorem. Compos Struct 207:519–530
15. Zhu P, Lei ZX, Liew KM (2012) Static and free vibration analyses of carbon nanotube-reinforced composite plates using finite element method with first order shear deformation plate theory. Compos Struct 94:1450–1460
16. Singh SD, Sahoo R (2020) Static and free vibration analysis of functionally graded CNT reinforced composite plates using trigonometric shear deformation theory. Structures 28:685–696
17. Garcia-Macias E, Castro-Triguero R, Flores EIS, Friswell MI, Gallego R (2016) Static and free vibration analysis of functionally graded carbon nanotube reinforced skew plates. Compos Struct 140:473–490
18. Wattanasakulponga N, Chaikittiratana A (2015) Exact solutions for static and dynamic analyses of carbon nanotube-reinforced composite plates with Pasternak elasticfoundation. Appl Math Model 39:5459–5472
19. Duc ND, Lee J, Nguyen-Thoid T, Thangd PT (2017) Static response and free vibration of functionally graded carbon nanotube-reinforced composite rectangular plates resting on Winkler–Pasternak elastic foundations. Aerosp Sci Technol 68:391–402
20. Lei ZX, Zhang LW, Liew KM (2015) Free vibration analysis of laminated FG-CNT reinforced composite rectangular plates using the kp-Ritz method. Compos Struct 127:245–259
21. Lei ZX, Zhang LW, Liew KM (2016) Buckling analysis of CNT reinforced functionally graded laminated composite plates. Compos Struct 152:62–73
22. Malekzadeh P, Zarei AR (2014) Free vibration of quadrilateral laminated plates with carbon nanotubes reinforced composite layers. Thin Walled Struct 82:221–232
23. Malekzadeh P, Shojaee M (2013) Buckling analysis of quadrilateral laminated plates with carbon nanotubes reinforced composite layers. Thin Walled Struct 71:108–118

24. Zhang LW, Lei ZX, Liew KM (2015) Free vibration analysis of functionally graded carbon nanotube-reinforced composite triangular plates using the FSDT and element-free IMSL-Ritz method. Compos Struct 120:189–199
25. Zhang LW, Lei ZX, Liew KM (2015) Buckling analysis of FG-CNT reinforced composite thick skew plates using an element-free approach. Compos B Eng 75:36–46
26. Zhang LW, Lei ZX, Liew KM (2015) An element-free IMLS-Ritz framework for buckling analysis of FG–CNT reinforced composite thick plates resting on Winkler foundations. Eng Anal Bound Elem 58:7–17
27. Farzam A, Hassani B (2018) Thermal and mechanical buckling analysis of FG carbon nanotube reinforced composite plates using modified couple stress theory and isogeometric approach. Compos Struct 206:774–790
28. Kiani Y (2016) Shear buckling of FG-CNT reinforced composite plates using Chebyshev–Ritz method. Compos B Eng 105:176–187
29. Kiani Y, Mirzaei M (2018) Rectangular and skew shear buckling of FG-CNT reinforced composite skew plates using Ritz method. Aerosp Sci Technol 77:388–398
30. Mehrabadi JS, Sobhani AB, Khoshkhahesh V, Taherpour A (2012) Mechanical buckling of nanocomposite rectangular plate reinforced by aligned and straight single walled carbon nanotubes. Compos B Eng 43:2031–2040
31. Wu CP, Chang SK (2014) Stability of carbon nanotube-reinforced composite plates with surface-bonded piezoelectric layers and under bi-axial compression. Compos Struct 111:587–601
32. Wang M, Li ZM, Qiao P (2016) Semi-analytical solutions to buckling and free vibration analysis of carbon nanotube-reinforced composite thin plates. Compos Struct 144:33–43
33. Karamanlı A, Aydoğdu M (2021) Vibration behaviors of two directional carbon nanotube reinforced functionally graded composite plates. Compos Struct 262:113639
34. Wang ZX, Shen HS (2011) Nonlinear vibration of carbon nanotube-reinforced composite plates in thermal environments. Comput Mater Sci 50:2319–2330
35. Guo XY, Zhang W (2016) Nonlinear vibrations of a reinforced composite plate with carbon nanotubes. Compos Struct 135:96–108
36. Quoc TH, Tu TM, Tham VV (2019) Free vibration analysis of smart laminated functionally graded CNT reinforced composite plates via new four-variable refined plate theory. Materials 12:3675
37. Fantuzzi N, Tornabene F, Bacciocchi M, Dimitri R (2017) Free vibration analysis of arbitrarily shaped functionally graded carbon nanotube-reinforced plates. Compos B Eng 115:384–408
38. Bisheh H, Alibeigloo A, Safarpour M, Rahimi AR (2019) Three-dimensional static and free vibrational analysis of graphene reinforced composite circular/annular plate using differential quadrature method. Int J Appl Mech 11(8):1950073
39. Shahrbabaki EA, Alibeigloo A (2014) Three-dimensional vibration of carbon nanotube-reinforced composite plates with various boundary conditions using Ritz method. Compos Struct 111:362–370
40. Wang JF, Cao SH, Zhang W (2021) Thermal vibration and buckling analysis of functionally graded carbon nanotube reinforced composite quadrilateral plate. Eur J Mech A Solids 85:104105
41. Zhang LW, Song ZG, Liew KM (2015) State-space Levy method for vibration analysis of FG-CNT compositeplates subjected to in-plane loads based on higher-order shear deformation theory. Compos Struct 134:989–1003
42. Zhang LW, Selim BA (2017) Vibration analysis of CNT-reinforced thick laminated composite plates based on Reddy's higher-order shear deformation theory. Compos Struct 160:689–705
43. Selim BA, Zhang LW, Liew KM (2016) Vibration analysis of CNT reinforced functionally graded composite plates in a thermal environment based on Reddy's higher-order shear deformation theory. Compos Struct 156:276–290
44. Wu CP, Li HY (2016) Three-dimensional free vibration analysis of functionally graded carbon nanotube-reinforced composite plates with various boundary conditions. J Vib Control 22(1):89–107
45. Lei ZX, Liew KM, Yu JL (2013) Free vibration analysis of functionally graded carbon nanotube-reinforced composite plates using the element-free kp-Ritz method in thermal environment. Compos Struct 106:128–138
46. Zhou D, Cheung YK, Au FTK, Lo SH (2002) Three-dimensional vibration analysis of thick rectangular plates using Chebyshev polynomial and Ritz method. Int J Solids Struct 39:6339–6353